EXPLORING THE APPLICABILITY OF DETACHED BREAKWATERS TO PREVENT EPHEMERAL INLETS IN NORTON POINT BEACH, CHAPPAQUIDDICK ISLAND, MA

A Dissertation
Presented to
The Academic Faculty

by

Ian Emerson

In Partial Fulfillment
of the Requirements for the Degree
MASTER OF SCIENCE in the
SCHOOL OF CIVIL AND ENVIRONMENTAL ENGINEERING

Georgia Institute of Technology
DECEMBER 2020

EXPLORING THE APPLICABILITY OF DETACHED BREAKWATERS TO PREVENT EPHEMERAL INLETS IN NORTON POINT BEACH, CHAPPAQUIDDICK ISLAND, MA

Approved by:

Dr. Kevin Haas, Advisor
School of Civil and Environmental Engineering
Georgia Institute of Technology

Dr. Hermann Fritz
School of Civil and Environmental Engineering
Georgia Institute of Technology

Dr. Jorge Macedo Escudero
School of Civil and Environmental Engineering
Georgia Institute of Technology

Date Approved: August 20, 2020

DEDICATION

During this trying year, I would like to thank the many individuals who made my thesis possible. My advisor, Dr. Kevin Haas, who provided many hours of instruction on both the wave theories underlying the GENESIS model and the exacting software package needed to run it.

Tom Dunlop, an author who has spent decades describing the coast of Martha's Vineyard. I lament the day, late in the thesis process, that I found his meticulously gathered notes that destroyed my initial hypothesis. Nevertheless, his newspaper and magazine articles exposed many details my maps and wave data missed: he reminded me that computing data thousands of kilometers away from your site is infinitely improved when you add in human eyes that have actually stepped on the sand.

Dr. Borja Sotomayor, Senior Lecturer of the Department of Computer Science at the University of Chicago, who aided the production of a better 2013 shoreline through his knowledge of interpolation. My roommate, Yogesh, who surrendered our kitchen table to my notes. Finally, my parents Donna and Geoffrey Emerson, for their tireless support through this all, and who also surrendered a table to my notes.

ACKNOWLEDGEMENTS

The scientists who previously explored the coast of Martha's Vineyard, both working with and at the Martha's Vineyard Coastal Observatory: Mara Orescanin, Steve Elgar, and Britt Raubenheimer: when the thesis author went looking off the coast of the Eastern United States for an inlet that a breakwater might aid, it was a mighty stroke of serendipity that the one he found had world-class sensors gathering wave, tide, and meteorological data nearby. It was another boon when the individuals who had previously used and tended that data were willing to speak with the author.

Chris Seidel, cartographer and GIS coordinator for the Martha's Vineyard Commission: Before, the author only had a lone set of data from 2013 and what he could scry from Google Earth images. With his assistance, he gained both a high-water shoreline and a comprehensive study of shoreline change in Massachusetts.

Silvia Di Bona, author of another master's thesis on the possibilities for a detached breakwater as modelled with GENESIS: internet searches for assistance on GENESIS do not yield great answers, but her previous application of the software to the Portuguese coast was an excellent reference.

TABLE OF CONTENTS

LIST OF TABLES

LIST OF FIGURES

LIST OF SYMBOLS AND ABBREVIATIONS

MVCO	Martha's Vineyard Coastal Observatory
MHHW	Mean Higher High Water
MHW	Mean High Water
MLLW	Mean Lower Low Water
MLW	Mean Low Water
MSL	Mean Sea Level
NP	Norton Point (Beach)

SUMMARY

Norton Point Beach connects the two halves of Martha's Vineyard, Massachusetts, but it has breached repeatedly in the past, allowing severe erosion of Wasque Point and disrupting transportation. Attempting to predict the breaches, the GENESIS and later the GENESIS-T models were applied to simulate the beach using USGS geographic data and Martha's Vineyard Coastal Observatory wave data. Unfortunately, the 1-D model proved to have limitations: the beach likely breached from the bay side of the modeled shoreline, and there was no direct data from inside the bay. Multiple configurations consistently overestimated erosion of the eastern side of the beach while overestimating accretion on the western side.

Simpler attempts to model the breach conditions support local belief that a number of factors, including a preceding winter of erosive high waves and an unusually high tide, combined to cause a major breach on April 17, 2007. The analysis does not support any coastal construction to directly prevent a breach, although a detached breakwater could still enhance accretion at certain parts of the beach.

After exploring various varieties of breakwater, a floating breakwater was determined to be the ideal candidate: new models can handle higher waves than before and change location, while its non-permanent nature makes it ideal for a region with strong opposition to offshore construction.

CHAPTER 1. INTRODUCTION

1.1 Barrier beaches and islands

Barrier islands and beaches are flat coastal landforms: they may first appear as a sand spit that slowly grows until it encloses a body of water behind it; alternatively, sea level may drop and expose an offshore sandbar (Uda, Serizawa, & Miyahara, 2018). In the case of a growing spit in the presence of a tidal inlet, one side may accrete while the other diminishes (Aubrey & Gaines, 1982). Should the enclosing beach erode at is connecting points, it will become a barrier island. In Massachusetts, the cyclical nature of these beaches defies the common conception of barrier islands constantly moving landward: groups of islands and beaches may exchange their sediment in a cycle of accretion and erosion while remaining in roughly the same place over human lifespans (World of Page: Coastline Change, n.d.).

1.1.1 Norton Point Beach

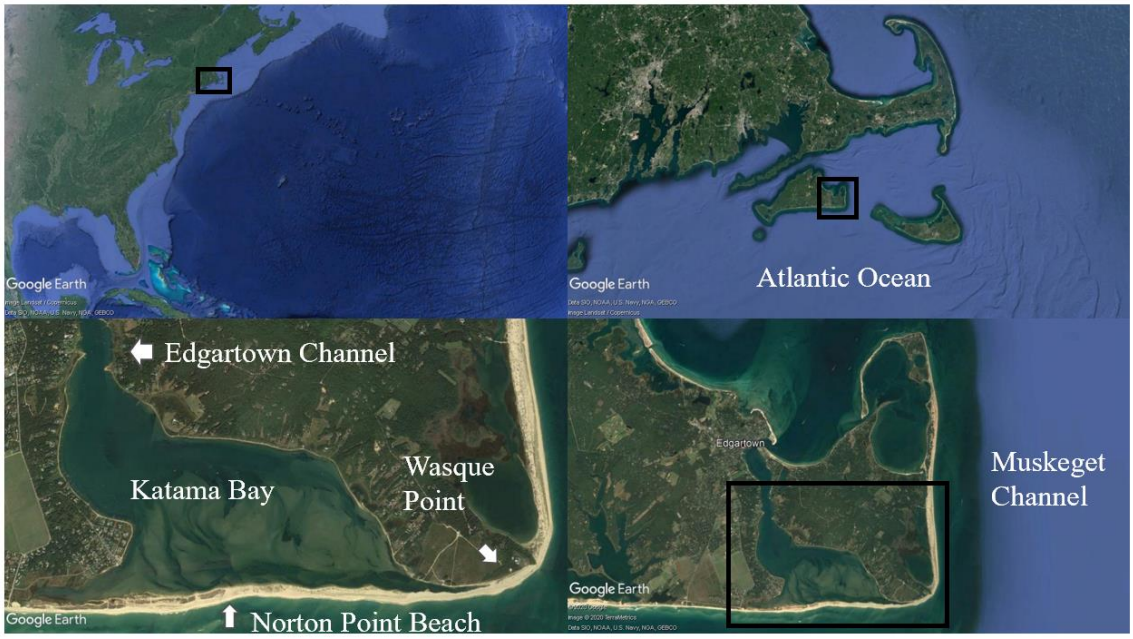

Figure 1. Clockwise from Upper-Left: Eastern United States, Massachusetts and its Islands, Eastern Martha's Vineyard/Chappaquiddick Island, Katama Bay and October 2018 Norton Point Beach (Google Earth, 2018-2020).

Martha's Vineyard is an island roughly 7 kilometers south of Falmouth, Massachusetts in the northeastern United States. As seen in Figure 1, it occupies roughly 250km^2 and is dotted with multiple lakes, ponds, and bays. Within it, Edgartown Township occupies the eastern section and includes Chappaquiddick Island, which despite the name is often attached to the rest of Martha's Vineyard by a narrow beach in the south known as Norton Point (NP) Beach. To the south of this beach, also sometimes known as part of Katama Beach, is the Atlantic Ocean, and to the north between Chappaquiddick Island and the main island is Katama Bay, roughly 5km^2 and less than two meters deep for most of its area. To the west of the bay is the Katama residential neighborhood. The Edgartown Channel that

leads to the Vineyard Sound in the north is deeper than the bay, reaching 8 to 10m before the open sea.

NP Beach has been repeatedly breached throughout human occupation of the island, usually only briefly, but sometimes for years. The last major breach as of July 2020 occurred during the Patriot's Day Storm in the early morning hours of April 17, 2007 (Dunlop, 2014).

Sampled from Google Earth images at multiple eastings between December 2000 and February 2018, NP Beach is usually between 70 and 95m from north to south. The fastest erosion in all of Massachusetts at the southeastern tip of the island, known as Wasque Point (Massachusetts Shoreline Change Browser, n.d.). With the disappearance of several defining ponds and cyclical erosion and accretion drastically reshaping the area, there is no concrete divider between NP Beach in the east and Wasque Point in the west. The barrier beach was roughly 3.5 km at its longest in the 2000s and 4 km in the 2010s.

Geologically, the island is

> "comprised principally of glacio-fluvial outwash sediments seaward of the terminal moraine on the north and east sides of the island, deposited during the last glaciation ca. 23 ka. These outwash plains are dissected by southward-trending valleys, presumably formed by spring sapping." (Goff, et al., 2005).

Storms may be a destructive force eroding beaches during the harsh winter, but overwash during intense storms can move sediment behind the berm. When wave run-up deposits sediment-filled water on the backbarrier it is often fan-shaped and described as "washover fan"; if they join together, those fans may form a "washover terrace". There have been three events in the past three decades resulting in overwash: two during 1991's Hurricane Bob, and one during a 1997 nor'easter. The sparsity of these events may explain the

shrinking of the beaches in the south of Martha's Vineyard, as without sufficient overwash there is no long-term equilibrium (Carruthers, Lane, Evans, Donnelly, & Ashton, 2013).

Twice a day, strong tidal currents run through the Muskeget Channel shown in Figure 1 on the eastern side of Chappaquiddick Island and up against the swiftly eroding Wasque Point. In 2003, the NNE current was 1.4 meters per second, while the SSE current was 1.6 meters per second (Tidal Currents through Vineyard and Nantucket Sounds, 2003). While 2006 EPRI research has the flood at typically 2 m/s and the ebb 1.7m/s, 2013 UNH research has placed the maximum observed tidal current at 2.5m/s (Previsic, 2016; Dewhurst, 2013).

Culturally, Martha's Vineyard and neighboring Nantucket are long famous for their fishing grounds, which continue to attract many for recreational fishing, as well as whaling, which was largely discontinued in the 1870s with the rise of petroleum and early sea ice trapping whaling vessels (Dunlop, Riches of Whaling Industry Came to Frigid End As Vineyard Captains Lost Ships Off Alaska, 1999). Today, tourism supplies both a majority of jobs on the island as well as driving the use of NP Beach (Economic Profile of Martha's Vineyard, n.d.).

Along with the reputation for whalers also came the famous shoals: although Nantucket's are more famous for endangering ships, the area off Wasque Point also changes shape and depth regularly, and just south of the breach in 2013, bathymetry becomes highly irregular (A Fine Load of Codfish, 1878; Andrews, Baldwin, Sampson, & Schwab, 2018).

1.2 Ephemeral Inlets

As previously mentioned, barrier islands are both nurtured and nipped at by storm activity. At times, the storm surge can combine with high wave activity to pierce through the barrier (Buynevich & Donnelly, 2006). This may not only result in the transport of sediment but the formation of a tidal inlet, allowing dramatic changes that ignore long-term trends in shoreline evolution (Buynevich & Donnelly, 2006).

> "Inlets are often carved from a surge of water flowing from behind the barrier towards the ocean. The oceanward flow of water from the back barrier region is often aided by offshore winds. During a storm surge, large volumes of water are forced into the back barrier region by overtopping waves, overwash, and inlet flow. As the storm recedes only the inlet provides access for the escaping flow. If the level of water in behind the barrier is high relative to the ocean side the inlet may be insufficient to provide drainage and the water will flow seaward through a weak point in the island creating a new inlet.
>
> Weak points that become sites of inlet formation occur where the barrier has been thinned and/or where foreshore wave activity has breached the foredune ridge and created washovers." (Inlets, n.d.).

In the case of breaching Katama Bay, Edgartown Channel already supplied tidal variation from the north, but this did not prevent the ebb and flow from maintaining the inlet after the Patriot's Day storm: rather, the channel flow was quickened and amplified.

1.2.1 History of Breaches

As the name implies, Chappaquiddick Island is only occasionally connected to the main island throughout its inhabited history. As seen in Table 1, NP Beach has been broken in eastern, central, and western locations multiple times since 1776. Usually these breaches last only days or weeks: due to the unremarkable nature of minor breaches to locals, not all

Table 1. Known or Suspected Breaches of Norton Point Beach (Dunlop, REVISED: A HISTORY OF THE OPENINGS (AND CLOSINGS), 2014; Dunlop, The Norton of Norton Point, 2011; Dunlop, An Eyewitness Account as the Beach Gives Way, 2011; Hurricane Bob Roared, and Martha's Vineyard Shook, 2016; Dunlop, Short-Lived Breach at Norton Point Closes, 2015; Wells, Norton Point Breaks Open Again on Stormy, Windswept Day, 2016; Brown, 2016; Wells, Northeaster Leaves Island in Cleanup Mode, 2018; Brennan, 2018; Dunlop, Man's Efforts to Open – and Close – Norton Point, 2011).

Start Date	Location	Notes	Natural?
1776	East	From Des Barres Map	Yes
1795	West	At Wasque End - Benj. Smith Survey	Yes
1830	West	Near Wasque. H. Grape Survey	Yes
1846	East	H.L. Whiting	Yes
1856	West and East	H.L Whiting. Possibly from a January 5-6 blizzard, but there is conflicting data on if there was a breach at this time. Similar conditions to 2007 breach noted in Vineyard Gazette, with an uncommonly high tide after a winter of strong storms.	Yes
1860	West and East	Unidentified hydrographic chart - possibly same breach as 1856	Yes
1871	Unknown	No opening from H.L. Whiting data	Yes
Fall 1873	East	Shell fishermen wanted the bay refreshed, and commercial fishermen wanted a shortcut to the rips off Wasque Point at the eastern end of Chappaquiddick. The effort involved an outlay of $20,000. Channel was dug from the bay outward. Overnight storm undoes work and closes the beach before completion.	No
1886	Unknown	"the Atlantic beach needed a new name after a storm broke through it in early January of 1886."	Yes

Table 1 (continued).

Start Date	Location	Notes	Natural?
Spring 1921	West/ Central	Migrated Eastward and closed sometime after 1924	Unknown
April 1932	Unknown	Intended to improve the shellfish conditions and provide work during the Great Depression.	No
1938	Unknown	Unknown	Yes
February 15-16, 1953	Unknown	Possible precursor to 1954 Breach	Yes
August 31, 1954	Unknown	**Hurricane Carol -** Ogden described the ocean surf still washing over Norton Point as he walked along the beach after the storm: At first, he wrote, the water streaming from Katama Bay was no more than two to four meters wide and less than thirty centimeters deep. But it "rapidly widened and deepened to produce a sand cliff near where I stood, 2–3 m high and a channel at least 50 m across....Within 2 hr of the first breach of the beach by ocean waves, the new opening was almost 300 m wide, and water was boiling seaward from Katama Bay. The following morning, under clear skies and a bright sun, the opening looked as if it had always been there, and the tide was flowing quietly into the bay from the ocean."	Yes

Table 1 (continued).

Start Date	Location	Notes	Natural?
August 19, 1991	Unknown	**Hurricane Bob -** "Many south shore ponds, including Katama Bay, rose several feet during the surge and broke through to the sea — part of the natural process of shoreline change."…but bay shoreline is continuous by the shore survey published for 1995. Researchers at the Martha's Vineyard Museum report that the beach was "altered" but not necessarily breached in the sense of a temporary inlet.	Yes
September 30, 2015	East	"During a storm on Sept. 30 the beach broke open again, just west of Wasque Point, severing Chappaquiddick from the main Island"" ...opposite the fishermen's parking lot. The pattern was the same as the 2007 opening: astronomically high tides, overwash softening up the beach, and the tide starting to fall in Edgartown as it was already falling at Wasque Point. The time was between 2:30 and 3 p.m." Closed on October 17th.	Yes
January 10, 2016	East	"the ribbon of sand" almost certainly refers to the short, slender piece of beach in the east that was the last part of the great breach's healing	Yes
March 3, 2018	East	Source article says early morning, so could have been late 3/2/2018…storm was going on then. Not present on 10/5/2018 Google Earth image. Likely lasted days or weeks; no more newspaper articles on it, and by June 6th driving permits were allowed, which are generally only offered when the beach is contiguous	Yes

openings (or especially closures) have been recorded in the local newspapers or commented on by scientists. Before the 2007 breach, the last breach to last over a year was in 1954, which itself may be from a small breach from 1953. Hurricanes unsurprisingly are associated with a large number of breaches, but they are by no means necessary. Human attempts at opening the breach tend to be quickly closed: just to the west of Katama Bay is the Great Pond, which is intentionally breached 4 times a year to promote the health of the water body, but there is no flow from the North to keep those breaches open, and the Great Pond Foundation often hopes for the openings to last just two weeks (though they often close sooner) (Elvin, 2015). Those breaches often end the same way as Dunlop describes NP breaches ending:

> "According to the Gazette and studies going back to the 1870s, most of these openings behaved in remarkably similar ways: A storm opens the beach and the inlet begins to migrate eastward with the longshore current toward Chappaquiddick. Once it reaches Chappy, tides and currents move the beach of Norton Point offshore, creating a tidal channel between the beach and Chappy as the point continues to grow to the east. The opening finally encounters new tidal forces at Wasque Point where, over time, it closes.
>
> But as the opening approaches Chappaquiddick, history and contemporary experience show, the inlet prevents "sediment transport" — migrating sand — from reaching the beach along the southern Chappy shoreline. The beach wastes away..." (Dunlop, History and Science Tell of Cycles of Rapid Erosion at Wasque Point, 2013).

1.2.1.1 Pros and Cons of Breaches

There are economic considerations when a breach affects a heavily populated or vital site. Corrective beach fills have a set cost on their own, but there is the added cost of haste and disruption by the tide when filling this breaches, as FEMA encountered addressing the damage and temporary inlets formed by Hurricane Sandy in 2012 (Velasquez Montoya, Sciaudone, Mitasova, & Overton, 2018). In August 2011, the storm surge of Hurricane Irene caused the Pea Island Breach in North Carolina (ibid). Because of the importance of

highway NC 12 as a lifeline in the Outer Banks, the NC DOT constructed a temporary bridge in the region, although they allowed the inlet to close naturally, which it essentially did in May 2013 (Harrison, 2010).

In Massachusetts, there is conflicting and changing opinion on the islands as to whether NP Beach is best closed or open. The beach has been opened by storm and by shovel a) to benefit the shellfish industry within Katama Bay, and b) to flush out refuse dumped or pumped out of harboring boats, but shellfish harvesters have also rejoiced at improved flavor when the beach finally closes (Elvin, Norton Point Breach Closing Benefits Birds, Shellfish, 2015; Katama Bay Oysters, n.d.; Lovewell, 2005).

When there is a breach, rather than the calm ebb and flow usually through the Edgartown Channel, there is a strong if cleansing tidal current cutting through the islands. People are placed at risk when trying to cross the beach in pitch black conditions (Dunlop, Special Report: Norton Point Breach, 2011). When a breach is predicted, or at least stable and advertised, fewer people are at risk from land vehicle accidents, although this itself does beget risk from increased boat travel.

On the negative side, increased erosion at Wasque Point occurs when the area is starved of sand that cannot cross the inlet; property and economy-supporting recreation are endangered. There is always a ferry to move people between Martha’s Vineyard and Chappaquiddick, but even when people would already use a ferry to cross, the presence of the breach increases the flow across the Edgartown Channel, making navigation difficult.

1.2.1.2 Human Solutions for Breaches

While there is plenty of literature on the use of breakwaters and other means to generally increase accretion on beaches, barrier and otherwise, there is little specifically published on preventing or reducing tidal inlets. In exploring situations for the coasts of Louisiana, Campbell describes

> "Two-Sided Nourishment: Placing sand and fine sediment to restore beach and marsh; dunes and berms built with consistent elevations during nourishment projects can reduce the potential for island breaching" (Campbell, Benedet, & Thomson, 2005).

He also mentions adding marshes and generally reducing the size of the tidal prism to promote natural closure.

Flood barriers can address storm surge if the affected site is already somewhat constrained and sheltered from the open ocean, but the immense cost of these barriers places them out of reach for many sites.

Although explored as a negative (as the inlets were already well-established), Davis and Barnard explored the effects of anthropogenic activities on tidal inlet stability (Davis & Barnard, 2000). The extensive construction in Florida of the 1920s to 1960s connecting barrier islands to the mainland added a great deal of choking sediment to these inlets.

1.2.2 Patriot's Day Breach

The April or Spring Nor'easter of 2007, also known in New England as the Patriot's Day Storm, was a powerful storm that dumped 20 centimeters of rain in some places and 50 centimeters of snow in others (NOAA, 2007). By April 2007, NP Beach had been intact

with no reported breaches for almost 30 years. There was a reported breach in August 1991 from Hurricane Bob, but LANDSAT images cannot confirm a breach even a week later on August 26th (Landsat Images on GloVis, 1991).

Once open, the breach slightly drifted eastward then expanded slightly until 2008, when it expanded sharply. As seen in Figure 2, it then began a progressive move to the east. Dunlop notes the breach closed overnight April 1st to 2nd, 2015. The narrow strip of land would be briefly pierced over the next few years, but nothing compared to the initial breach in size or duration.

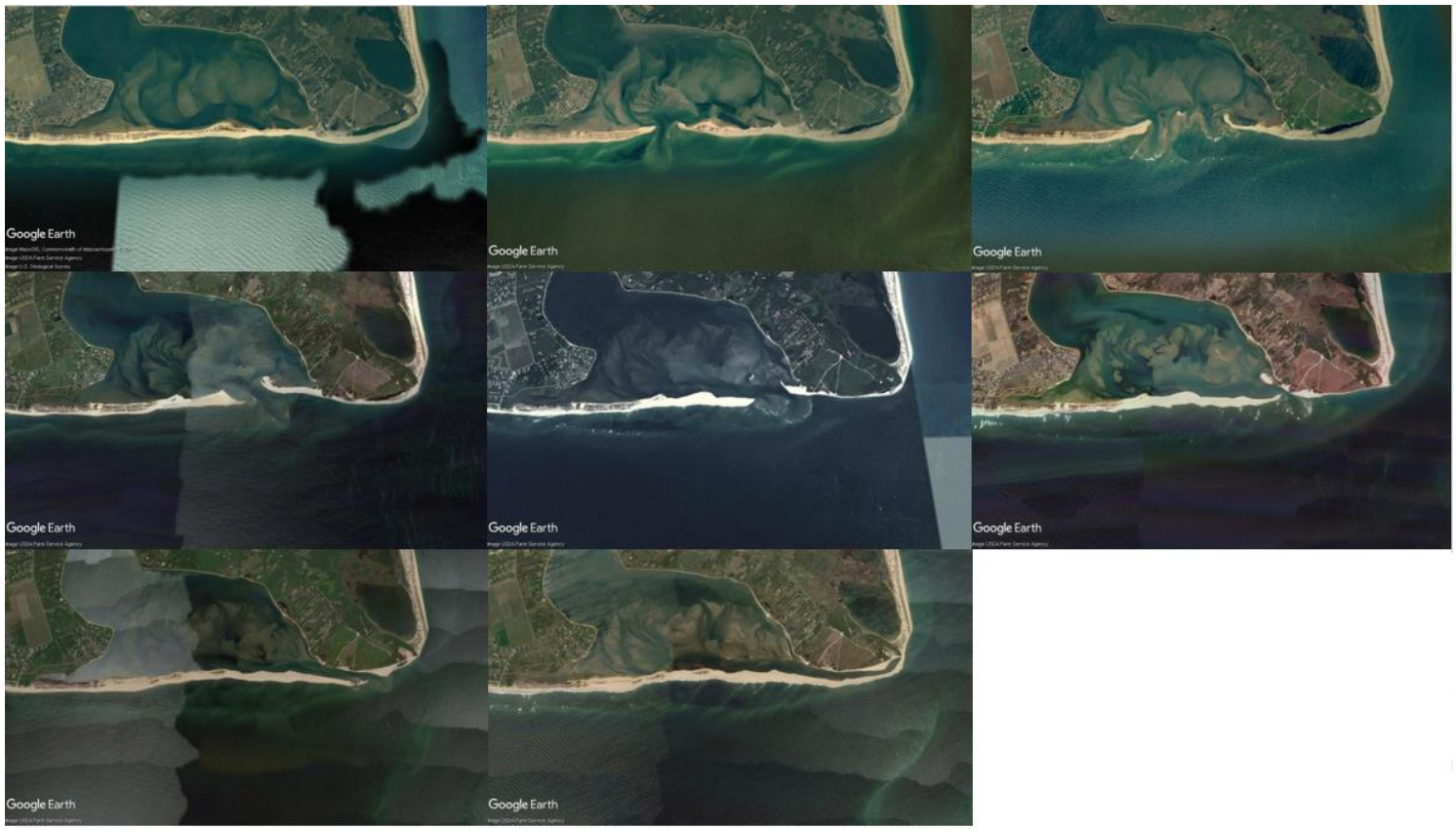

Figure 2. Images of NP Beach. From Left to Right and Top to Bottom from Upper-Left: 2005, 2007, 2008, 2010, 2011, 2012, 2014, 2015. Note that the last image is just about a month after the breach healed. (Google Earth, 2005-2015).

Although the rest of this study documents the breach from instrument data, eagle-eyed observers such as Tom Dunlop have watched the area for decades and provided essential background information. Dunlop's claims on breach causes are as follows:

"• A great storm came up from the south, with winds and seas battering South Beach from the southeast for several days.

• The beach itself was low, narrow and often overwashed after a winter of damaging storms.

• There was an exceptionally high tide in Katama Bay on the night of April 16-17, caused by a full moon at its closest approach to earth that year.

• The wind veered to northwest as the tide fell in the Atlantic just before midnight on April 17. But the water in the bay remained exceptionally high. As the last storm waves overwashed Norton Point, the pressure of the water seeking to escape the bay during the falling tide there drove the waters outward, creating the new opening" (Dunlop, REVISED: A HISTORY OF THE OPENINGS (AND CLOSINGS), 2014).

He also provides an eyewitness account:

"On a misty, windy morning in April 2007 Chris Kennedy, Martha's Vineyard superintendent for The Trustees of Reservations, had just returned from the part of South Beach in Edgartown known as Norton Point.

The night before Katama Bay had filled to overflowing by the flood of an astronomical high tide, topped off by the overwash and storm surge of a Patriots' Day gale. On the south side of Norton Point relentless, reaching ocean waves had flattened, narrowed and weakened the barrier beach. With the fall of the tide on the ocean side shortly after midnight, the beach had broken open to the Atlantic. Water in the bay had rushed out to the ocean, severing Chappaquiddick from the rest of the Vineyard for the first time in 30 years but restoring the word 'island' to its name as well as its spirit.

The channel through the beach was only a few hours old, but it was already more than 200 feet wide. 'This clearly is a major breach,' Mr. Kennedy told the Gazette that Tuesday morning, April 17, 2007. 'It's really something to see, just the sheer volume of water rushing through there. I don't think this thing is going to heal over in the short term.'

He also said: 'This is not a catastrophe. It is simply Mother Nature at work.'" (Dunlop, History and Science Tell of Cycles of Rapid Erosion at Wasque Point, 2013).

1.3 Goal of This Study

Norton Point Beach has breached in the past and it will almost certainly breach again. While small, brief breaches may be beneficial, and even large ones may have their benefits, the inhabitants of Chappaquiddick and Martha's Vineyard will definitely benefit if they can predict when breaches will form and how long those breaches will last. Should the harm of the breach be great, they will also benefit from tools that can prevent breach formation or at least speed breach closing.

For prediction, the thesis author will try to use the GENESIS or the similar GENESIS-T model to hindcast the beach for the years right before the breach, then apply it to the breach period. A sudden increase in erosion at the expected Patriot's Day breach location will suffice, as GENESIS cannot model the effects of Katama Bay on its northern side.

The GENESIS model may fail, and a second predictive approach could both confirm model predictions and/or be useful on its own. Therefore, the thesis author will explore if examining wave heights and storm surges, both as individual readings and seasons/years, can predict breaches. As local area observer and author Tom Dunlop states four reasons that made the Patriot's Day Breach likely, those claims will also be verified.

Although a legitimate engineering project would explore both soft and hard coastal engineering solutions for preventing or healing breaches, this paper will only explore detached breakwaters. New advances since the dominance of soft engineering may be generally underapplied and beach nourishment could have unwanted effects on already-shallow Katama Bay. Although the study will not go as far to as to sketch out a

prototype, there are twin goals of a final suggested style and preliminary calculations for armor blocks.

CHAPTER 2. DATA SOURCES AND PROCESSING

Almost any coastal engineering model will require local bathymetry and topography, as well as wave information. Tide and sea level data was used to evaluate storm surges, and wind data was also gathered to narrow down when "storms" occurred as described in newspaper articles about breaches.

Although they are not described further below, Google Earth and Landsat images of the region were also useful for observing the evolution of the breach. In the latter's case as seen in Figure 3, they supported a 2018 report of a minor breach in the east, though the image was of extremely low quality.

Figure 3. Landsat Image of Minor NP Beach Breach from March 14, 2018 (Landsat Images on Glovies, 2018).

2.1 Waves

Figure 4. Martha's Vineyard Coastal Observatory Node Relative to NP Beach, taken December 2008.

The wave data comes from the Martha's Vineyard Coastal Observatory. Based in Edgartown with an offshore wave sensor in 12m deep water south of Martha's Vineyard, the wave data goes back to 2001, although the data becomes much more reliable starting in 2002.

For use in GENESIS and other analyses, the wave data was processed with Python to remove the gaps, average the usually-every-twenty-minutes data into 6 hour readings with significant wave height, period, and direction, and use a three-year (more if required)

average for a particular date and time to fill in any remaining gaps to produce 25011 wave records covering 2001 to 2018.

Table 2. Example of Raw Wave Input (Some Columns Omitted).

Year	MO	D	H	M	S	height [m]	period [seconds]	dir [degrees]	tide_paros [m]
2007	4	10	3	0	0	NaN	NaN	NaN	-0.09
2007	4	10	3	20	0	NaN	NaN	NaN	-0.05
2007	4	10	3	40	0	NaN	NaN	NaN	-0.03
2007	4	10	4	0	0	NaN	NaN	NaN	0.02
2007	4	10	4	20	0	NaN	NaN	NaN	0.04
2007	4	10	4	40	0	NaN	NaN	NaN	0.07
2007	4	10	5	0	0	NaN	NaN	NaN	0.09
2007	4	10	5	20	0	1.4	22.4	173	0.09
2007	4	10	5	40	0	NaN	NaN	NaN	0.07
2007	4	10	6	0	0	NaN	NaN	NaN	0.07
2007	4	10	6	20	0	2.1	28.8	177	0.02
2007	4	10	6	40	0	0.8	9.3	NaN	-0.01
2007	4	10	7	0	0	1.8	26.7	158	-0.09

While 10 years of the raw data had less than 1000 rows with NaNs for height/period/direction, 2001 had over 7000. Table 2 above illustrates some of the gaps in the raw data: instrument notes detailing equipment failures and fouling explain some but not all of them. Although the rolling averages were fine for the occasional patch, 2001's information was almost entirely pieced together from these averages, and it was eliminated for the calibration and other GENESIS simulations that were started in 2002.

```
20020102 1200 0.9 3.9 238.0
20020102 1800 0.8 4.3 229.0
20020103 0 0.8 4.1 235.0
20020103 600 0.7 4.2 238.0
20020103 1200 0.4 5.1 208.0
20020103 1800 0.4 6.0 194.0
20020104 0 0.3 9.4 163.0
20020104 600 0.3 6.8 178.0
20020104 1200 0.4 8.3 176.0
20020104 1800 0.5 7.2 184.0
20020105 0 0.9 4.9 222.0
20020105 600 1.2 6.2 222.0
20020105 1200 1.1 5.5 225.0
20020105 1800 1.0 5.5 226.0
20020106 0 1.1 5.3 217.0
20020106 600 1.2 5.3 213.0
20020106 1200 1.0 5.1 216.0
```

Figure 5. Section of Averaged Wave Data: Date, Time, Height, Period, Direction.

When the raw, usually-every twenty minutes sampled with gaps in the data is used, it is hereby referred to as the **raw wave data**. When the file is used with gaps in the data removed and everything averaged into every-four-hours averages, **averaged wave data** is used, an example of which is seen above in Figure 5. If the dates covered by the data are not specified, assume the averaged wave data covers January 1st 2002 until September 5th 2018, as this was the file used for the vast majority of GENESIS simulations. Note: this file was usually run only until the 4^{th}, as the 5^{th} is incomplete.

For the averaged wave data, the mean height was 1.0m with a standard deviation of 0.6m. The mean period was 6.0s with a standard deviation of 1.9s; finally, the mean direction was 188° (coming out of the south-south-west), with a standard deviation of 31.1°.

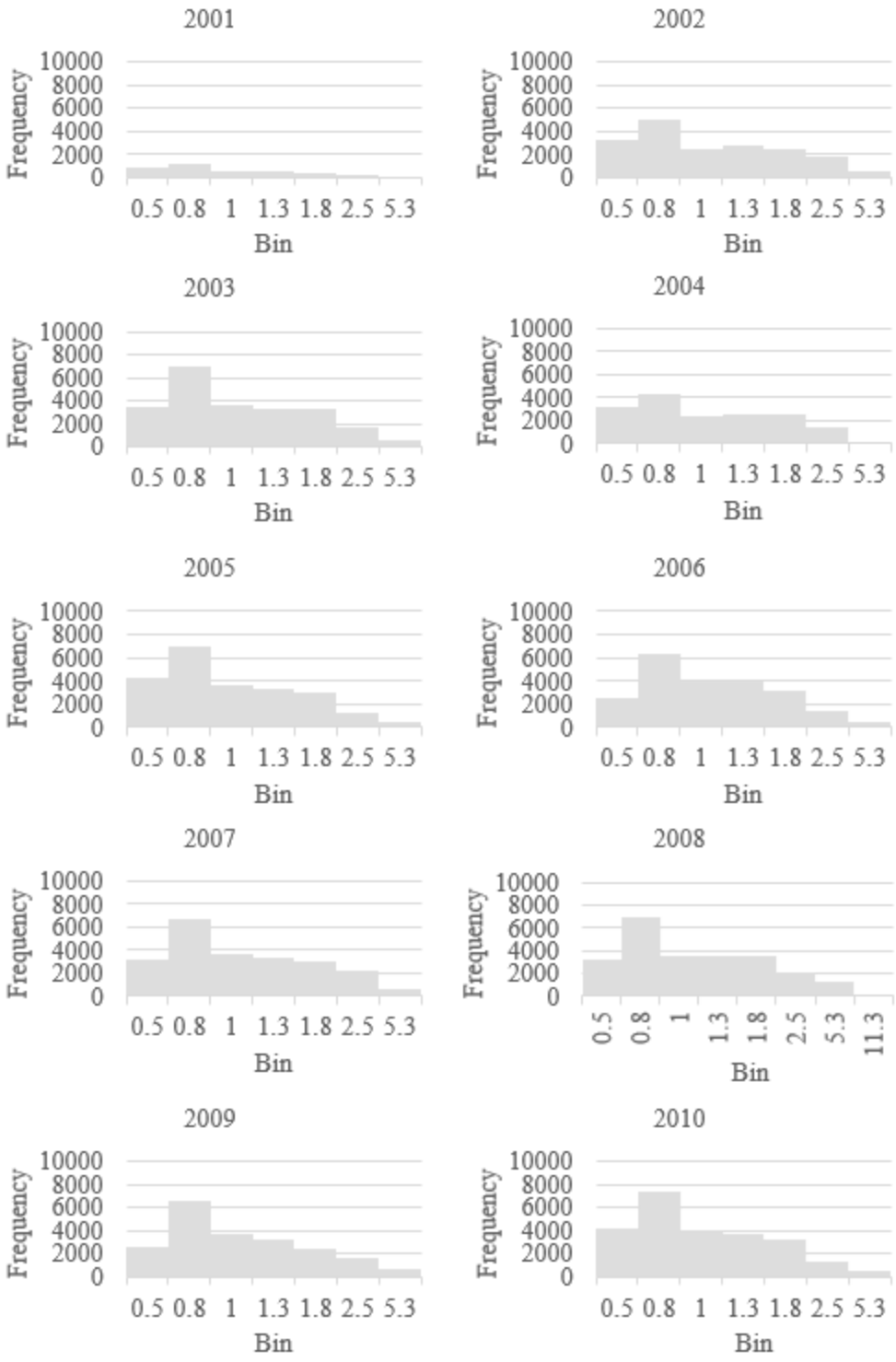

Figure 6. Histograms of Raw Wave Height Data, 2001-2018.

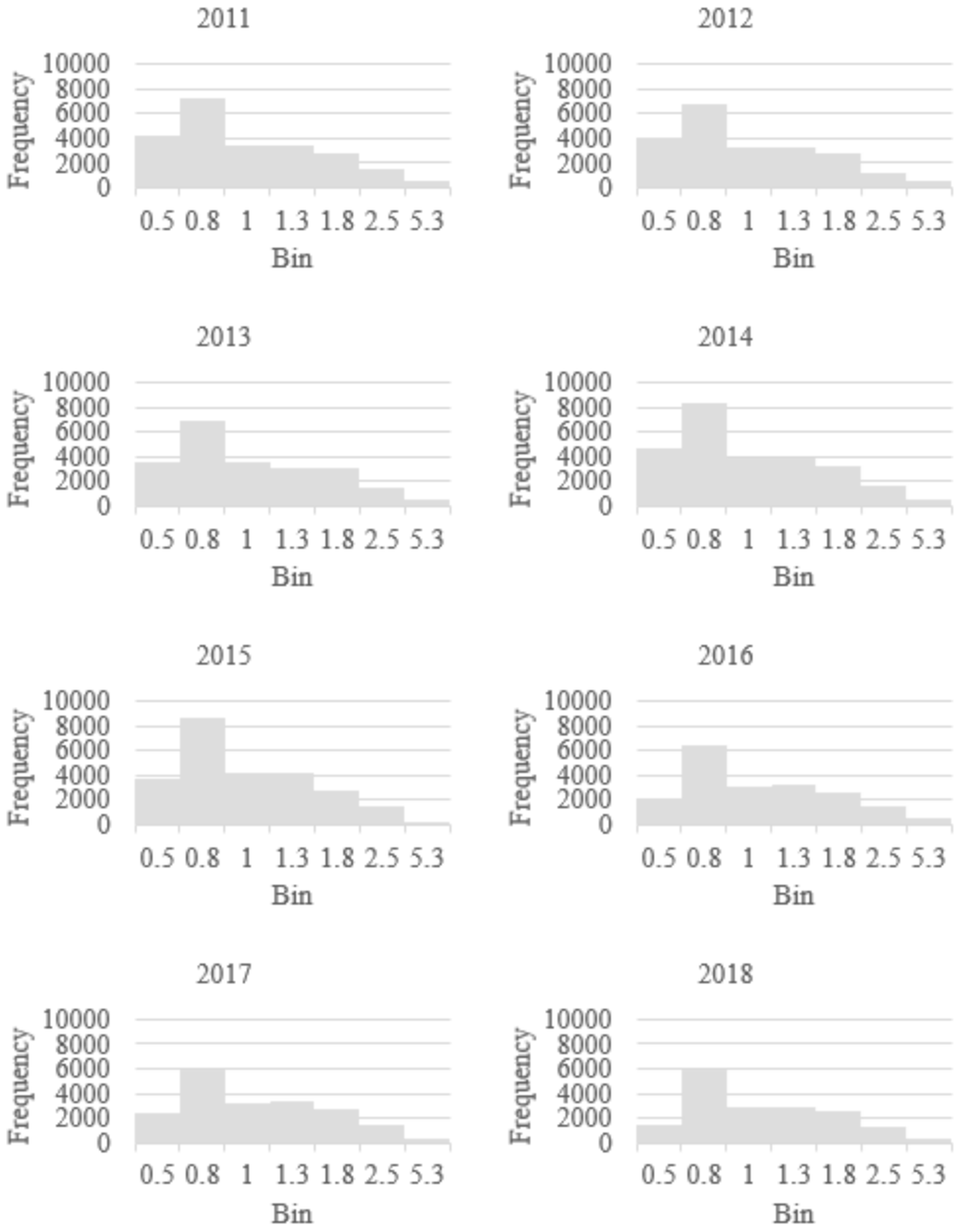

Figure 6 (continued).

Figure 6 above shows the variation in significant wave heights by year. For all years 0.51-0.8m waves form the most common band, and the number of waves in bands above 2.5m were highly variable.

2.2 Wind

Although not used in GENESIS, meteorological data also comes from the Martha's Vineyard Coastal Observatory (MVCO). Wind data was examined for a stricter definition of "storm" in the history of the island.

2.3 Tides

Although the PAROS instrument on the MVCO node provides information about sea level height by adjusting the total pressure and removing the atmospheric pressure, true NOAA tide gauge information from nearby Nantucket and Woods Hole was used for comparison. Although there was a tide gauge in in Edgartown, NOAA records only exist for about a month in 2004. The Edgartown gauge was near the permanent northern inlet to Katama bay, as seen in Figure 7.

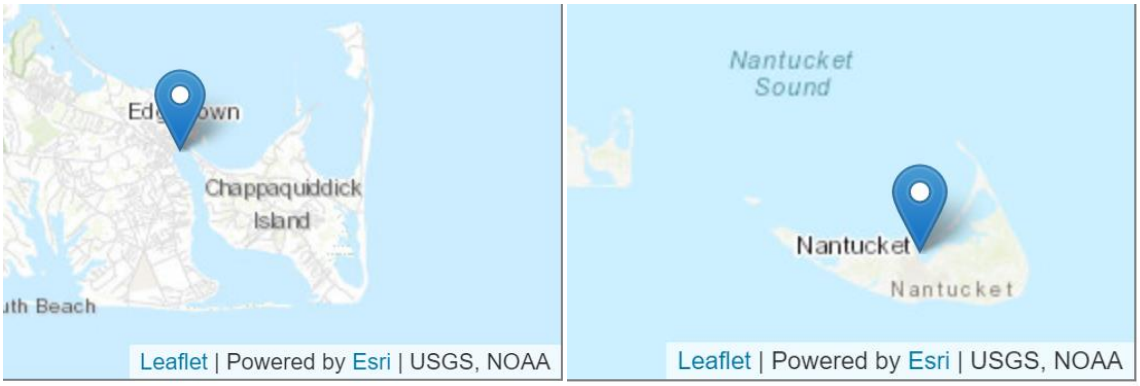

Figure 7. Location of Edgartown (left) and Nantucket (right) tidal gauges (USGS, NOAA).

2.4 Bathymetry/Topography

USGS provided the combined bathymetry/topography data from May to June 2013 (Andrews, Baldwin, Sampson, & Schwab, 2018). The data was provided as a GeoTIFF in UTM 19, NAD 83, NAVD 88 standards. This massive file was converted with QGIS to the XYZ format used, then trimmed using Python so as not to later crash the Grid Generator program. This XYZ data would also be used for determining berm height, producing approximate shorelines, and all other tasks requiring accurate topography/bathymetry.

Google Earth provided irregularly timed satellite images during the time period in question; since the dates it provides do not provide the time of day, the images cannot directly show how much erosion has occurred. An image at high tide could in some places falsely demonstrate a 50-meter change if the previous image was taken at low tide. However, the example below shows how the thesis author calculated the limits of this uncertainty, in order to locate the locations with low uncertainty for calibration purposes.

By NAVD88 at Edgartown MHHW is 0.236m and MLLW is -0.58m. Narrowing down the bathymetry to eastings where the northings containing both depths are closest yields easting 374905 as seen below in Table 3.

Table 3. Bathymetry Excerpt for Calculating North South Uncertainty, UTM.

Easting (m)	Northing (m)	Depth (m)
374905	4578518.014	0.657407
374905	4578508.014	0.698643
374905	4578498.014	0.238873
374905	4578488.014	-1.2428

0.236m surpasses 99.8% of the difference in depth between the last two northings, and -0.58m surpasses 39.1%. This equates to 9.98m and 3.91m estimates northing differences from the last northing, or 6.1m. This is the uncertainty when eyeballing erosion and accretion through Google Earth images at easting 374905.

Combining bathymetry with tidal range data allows for estimating the maximum error as seen in Table 4; if in one place the tide exposes and covers 50m of beach per day, and in the other only 10m, then the later will a better calibration point.

Table 4. North-South Uncertainty in Google Earth Images, Calculated from Possible Tidal Ranges, Meters.

Easting Location	2004 Edgartown Range (1.127m)	MHHW/MLLW Edgartown Range (0.816m)	PAROS Range (1.31m)
376385	47.1	41.3	50.3
376395	48	41.6	51
375855	49.3	43.8	52.4
374905	9.2	6.1	13.7

CHAPTER 3. GENESIS-T MODEL AND PROCESSING

3.1 Model Basics

The following is largely taken from the Army Corps' user manual on GENESIS (Gravens, Kraus, & Hanson, 1991):

The GENESIS model relies on a beach profile, the various depths and heights of sediment, that is focused between the top of active berm on land and the depth of control out at sea (more on depth of control in a later section). All sediment transport is assumed constrained between these two points, combined with another axis known as a one-contour line that is the length of the shoreline. Horizontal circulation is not directly considered, but net longshore sand transport rates are taken as a function of breaking wave height and direction. The model works well with wave-dominated shorelines, as opposed to tide or current dominated shorelines.

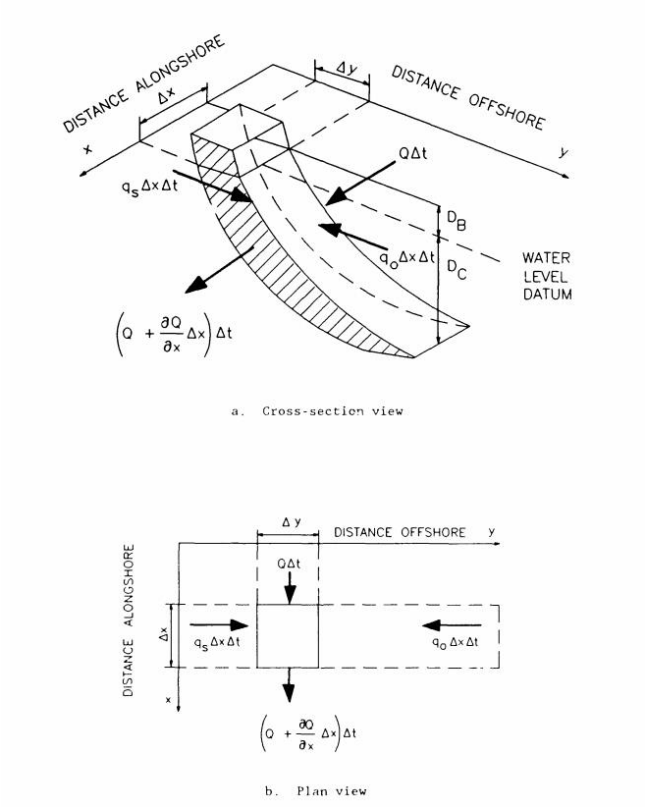

Figure 8. Definition sketch for shoreline change model (Gravens, Kraus, & Hanson, 1991).

The partial differentiation equation used, based on conservation of sand, is illustrated above in Figure 8 and with the following four equations. Equation 1 is the governing equation for the rate of change of shoreline position, and Equation 2 shows the longshore sand transport rate. Equations 3 and 4 shows the two non-dimensional parameters it uses, which themselves are based on k_1 and k_2. Much older concepts than GENESIS itself, many values of k_1 and k_2 are available from empirical experiments, but for accurate modelling those values are only starting points to fine-tune for the particular region.

$$\frac{\partial y}{\partial t} + \frac{1}{(D_B + D_C)}\left(\frac{\partial Q}{\partial x} - q\right) = 0 \quad (1)$$

Q is the longshore sand transport rate.

D_B is the height of the berm and D_C is the depth of closure.

q is the rate of removal or addition for a volume of sand per unit width of beach.

$$Q = \left((H^2 C_g)_b (a_1 * sin2\theta_{bs} - a_2 * cos\theta_{bs}\,(\partial H/\partial x)\right)_b \quad (2)$$

H is the wave height.

C_g is the wave group speed given by linear wave theory.

b is a subscript denoting breaking wave conditions.

θ_{bs} is the angle of breaking waves to the local shoreline.

$$a_1 = \frac{K_1}{16(S-1)(1-p)(1.416)^{5/2}} \quad (3)$$

$$a_2 = \frac{K_2}{8(S-1)(1-p)tan\beta(1.416)^{7/2}} \quad (4)$$

$S=\rho_s / \rho$, where the former is the density of sand (taken as 2.65 kg/m^3 for quartz sand) and the latter is the density of seawater (1030 kg/m^3 is used here).

tanβ is the average bottom slope from the shoreline to the depth of active longshore sand transport.

For determining the location of breaking waves for offshore structures such as detached breakwaters (which would have different breaking locations than in the natural beach profile), the water depth is approximated based on the median nearshore beach grain size as in below Equations 5 and 6.

$$D = Ay^{\frac{2}{3}} \tag{5}$$

$$A = 0.41(d_{50})^{0.94}, d_{50} < 0.4$$

$$A = 0.23(d_{50})^{0.32}, \leq 0.4\ d_{50} < 10.0 \tag{6}$$

$$A = 0.23(d_{50})^{0.28}, 10.0 \leq\ d_{50} < 40.0$$

$$A = 0.46(d_{50})^{0.11}, 40.0 \leq d_{50}$$

Two different submodels can supply wave data for GENESIS: internal, based on a simplified wave bottom and alignment, and external, based on wave transformation over the actual bathymetry of the area; if the wave does not break in the external submodel, it is processed by the internal model. The external submodel is attempted in all below simulations.

Support for detached breakwaters was added in the second version of GENESIS, which requires a transmission coefficient between 0 and 1 to account for wave behavior around an idealized breakwater. Only 2 x-, y-, and z-positions, along with this permeability can be explored in GENESIS: specific breakwater designs must be explored outside of the model.

The three main models mentioned before are broken down into two models: 2000-2001, and 2013. These are known hereafter as **Model A** and **Model B.** An earlier 2013-based model that was superseded by Model B, but below it may be referred to as the **pre-model** if necessary.

3.2 Pre-GENESIS Software Steps

3.2.1 Grid Generator

As the source bathymetry has a resolution of 5 meters, the grids were originally to be 10x10m. However, as the user manual only mentions 50ft (15.24m) as the lowest GENESIS resolution, and as a later decrease in time step necessitated increasing the grid size to reduce processing time, the grids used in the end were 20x20m.

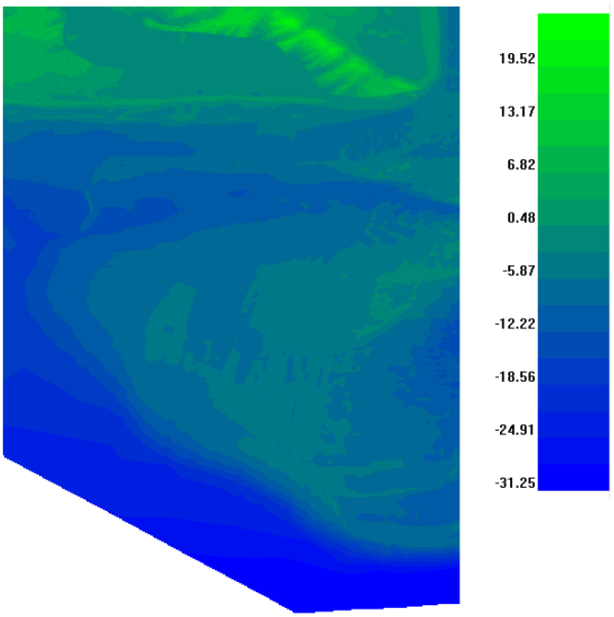

Figure 9. Trimmed Topographic and Bathymetric Data for NP Beach Area, NAVD88.

The area placed in the Grid Generator as seen in Figure 9 has west and east border of 373105 and 379120 (UTM 19). The northmost point is 4580820 and the southmost point is 4566810. The GENESIS spatial grid is a much smaller section of this at 4660m east/west and 4500m north/south. As the island is at a slight tilt, the azimuth of the grid was adjusted to 358 degrees.

The grid was chosen primarily to cover the east-west land area south of the bay. Additionally, Wasque Point was included not only because the erosion of Wasque is bound to the breached/unbreached nature of the beach, but also because the boundary between the point and NP Beach is ambiguous.

"Contour depth at first station" is set using 0.6 times the most extreme wave event, which at 11.3m yields 18.8m; 6.8m was used in the models below to significantly shrink the grid while covering the vast majority of waves, and test with 9.2m showed little difference (US Army Corps of Engineers, 2003).

3.2.2 Shorelines

Pre-model: For each 10m easting, all the bathymetry/topography readings between -0.75 and 0.75m depth were averaged to produce an approximate shoreline. This line was highly irregular, and produced a line based on 0m NAVD88, rather than the local mean sea level.

Model A: Source GIS Information was not operationally downloadable from the Massachusetts Shoreline Change Browser or the Martha's Vineyard Commission, but the Browser did allow a Google Hybrid Basemap. An image was overlain and scaled appropriately on Google Earth Pro, the line was traced with the path tool, the path was

exported and converted to UTM19 with QGIS, then finally being into the Grid Generator as seen in Figure 10.

Model B: For each 10m easting, search or interpolation produced the likely north-south position of the sea level at this point. The result is visible below in Figure 11.

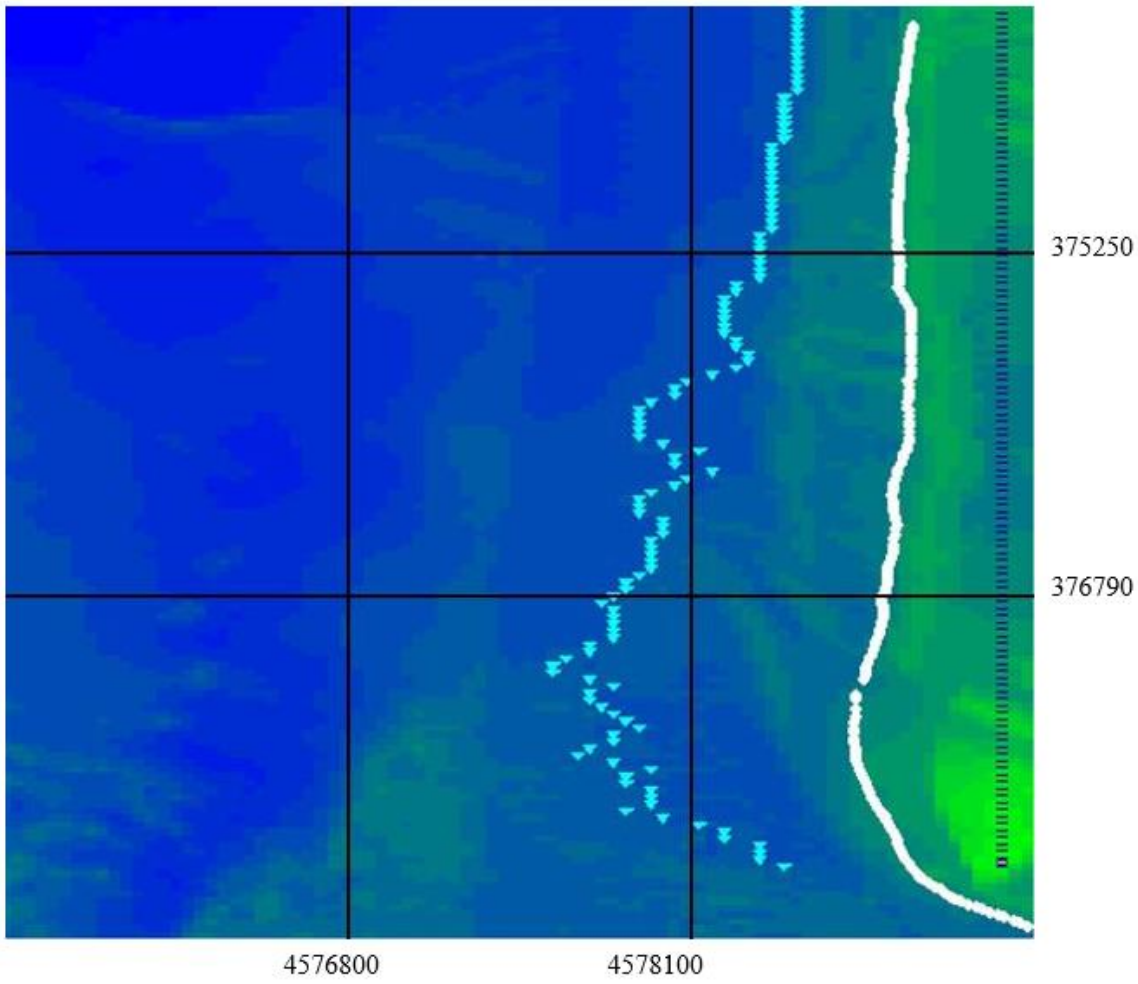

Figure 10. Model A. Norton Point Beach, UTM, Shoreline in White, Stations in Light Blue, Border of GENESIS Grid in Dark Blue.

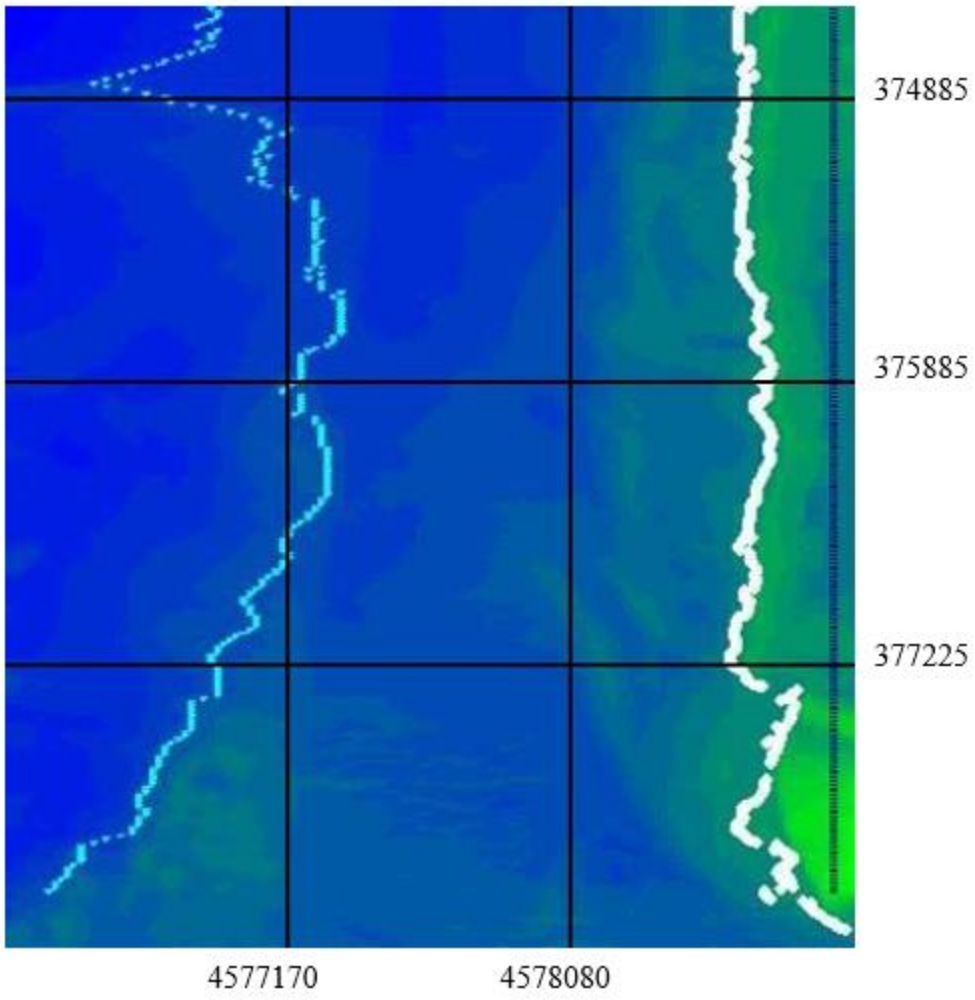

Figure 11. Norton Point Beach, UTM Markings, Shoreline in White, Stations in Light Blue, Border of GENESIS Grid in Dark Blue.

3.2.3 WWWL, First Pass

A new WWWL file is created, importing the averaged wave data and setting the index type to time. The mean water depth is 12 meters, the horizontal datum is NAD83, the vertical datum is MSL, and the World Coordinate System to UTM zone 19. The time setting is kept at GMT, the wave units are set to meters, and the direction convention is meteorologic.

Table 5. Important Direction Conventions for Wave Data Preparation.

Meteorologic/Meteorological	0 degrees is true north, describes direction **from which** wave is coming
Oceanographic	0 degrees is true north, describes direction **to which** wave is going
Shore Reference 1	90 degrees refers to a wave travelling parallel to the shore **from right to left**; -90 degrees, the same **from left to right**

3.2.4 WISPH3

WISPH3, seen below in Figure 12 is "a simplified point-to-point steady-state spectral transformation of WIS 2-component wave descriptions from deeper water to an arbitrary shallower water depth" that generates "theoretical directional spectra, performs shoaling and refraction, and considers shore-induced sheltering at a nearshore location" (CEDAS Details, n.d.). The output of the preceding WWWL is the input wave file, with the shoreline orientation now set to 90 degrees less than the original grid. In this case, 358-90=268 degrees. 12 meters remains the depth used.

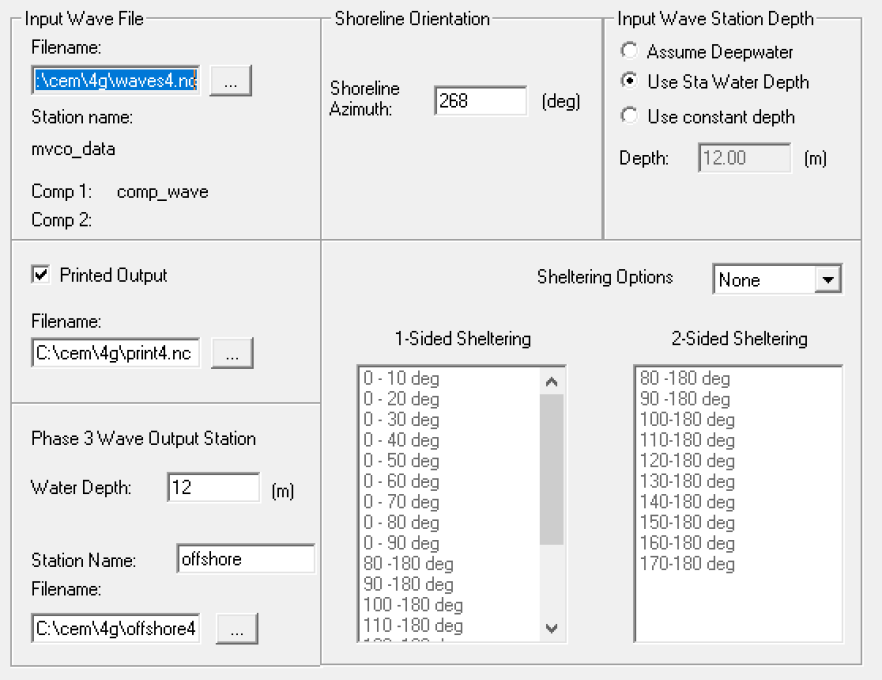

Figure 12. WISPH3 Screenshot.

3.2.5 WWWL, Second Pass

The output of the preceding WISPH3 step serves as input, and changing the direction convention, "shore_ref 1" is now used and the orientation is again set to 90 degrees less than the preceding step; 268-90=178 degrees.

3.2.6 WSAV

Processing tens of thousands of wave events with their own heights, periods, and directions would be computationally expensive, so here band limits are set for each category before saving the permutation results; The final limits chosen are shown in Table 6. Although initial band limits for preliminary models attempted the most normal distribution of wave qualities, this was later slightly amended to prevent the extremes from having undue

influence, e.g. all 4 to 11m waves being treated as 7.5-meter waves. Care should be taken not to use the raw meteorological direction to produce a normal distribution, as it has been shifted; fortunately, WSAV has built in viewing tools for viewing the distribution of the three qualities individually and in combination with each other.

Table 6. Band Limits Used For Processing Wave Data.

Height (m)	Period (s)	Direction (θ)
0	0	-90
0.5	4.1	-60
0.8	5	-46
1	6.1	-32
1.3	7	-8
1.8	8.1	6
2.5	9	14
6.9	11	22
11.3	45	30
	74	40
		52
		60
		75
		90

3.2.7 SPECGEN

SPECGEN "generates 2D directional wave spectra using [the] TMA (TEXEL storm, MARSEN and ARSLOE) parametric spectrum model combined with a cosine power spreading function" (Di Bona, 2013) Upon opening the software, the user can set the minimum frequency of interest (0.05Hz), the delta/fineness acceptable (0.01Hz), and the total number of bins/frequencies to be output (30).

3.2.8 STWAVE

STWAVE is "a 2-D finite-difference representation of a simplified form of the spectral balance equation to simulate near-coast, time-independent spectral wave energy propagation" (CEDAS Details, n.d.). Provided with the processed wave data from the previous steps, along with the grid and station data produced in Grid Generator, it can provide the external wave model used by GENESIS.

STWAVE is the lengthiest computational task of the shoreline simulation process; even with a 20x20m grid, the wave and station output were not ready for five hours, far longer than all other steps combined. A 10x10 grid took 9 hours, and an additional spectrum band for height and direction (to prevent outsize influence from outliers) increased runtime to 19 hours.

3.2.9 WWWL, Third Pass

To smooth the data for GENESIS use, all heights, periods, and directions are adjusted. The mean between each two bands is assigned as the value for all waves with values between the band limits.

3.3 GENESIS-T

3.3.1 Choice of GENESIS-T over GENESIS

Due to the ability for detached breakwaters to create tombolos, the initial GENESIS program was swiftly jettisoned for GENESIS-T. The chief difference is that GENESIS-T can account for tombolos, which while forming or completed can introduce "wave

diffraction, blocking of previously open calculation cells, and transport of sediment on both the landward and the seaward sides" of a detached breakwater (Hanson & Kraus, 2004).

3.3.2 GENESIS-T Settings

3.3.2.1 Depth of Closure

Three equations were considered for determining depth of closure: although a profile of the nearby sea is preferable, the irregular and changing bathymetry in the eastern half of the island complicated choosing which date's profile should be applied.

$$D_C = 2.28H_S - 68.5\left(\frac{H_S^2}{gT^2}\right), MLW \tag{7}$$

$$D_C = 1.75H_S - 57.9\left(\frac{H_S^2}{gT^2}\right), MLW \tag{8}$$

$$D_C = 8.9\overline{H_S}, MLW \tag{9}$$

The first is Hallermeier 1981 which yields a conservative answer and is generally the most recommended, the second is Birkemeier 1985, and the third is Houston 1995. For the first two, the wave height used refers to the significant wave height, in meters, exceeded 12 hours in a particular time interval (Kraus, Larson, & Wise).

The '81 gives 5.6m MLW, or 6.1m NGVD, which is used in these simulations. The '85 equation yielded 3.8m MLW, and the '95 was not used as the above Kraus guide says it was not applicable for a particular storm event. In retrospect, the entire GENESIS model was not meant for the effects of a particular storm event.

3.3.2.2 Berm Height

Five points were sampled and the highest point NAVD88 was used as the initial berm height, then adjusted to mean sea level. Eastings 374485, 375105, 375805, and 377105/377115 at their highest points were averaged together to produce 2.35m. Surprisingly, the highest berm height was found in the newly rebuilt eastern sections, although there was only about 10cm of variation between all the sample points.

3.3.2.3 Grain Size

A previous study investigated the sorted bedforms of the area and provided over 90 grain size samples (Detailed investigation of sorted bedforms, or ‘‘rippled scour depressions,’’ within the Martha’s Vineyard Coastal Observatory, Massachusetts). Offshore, there is a great amount of variation in the particle size that produces these depressions, seeming to complicate the decision to run a simulation with a single grain size. The earlier section on GENESIS and grain size shows the most important pertinent factor is if the grain size is below or $\geq$ 0.40mm; coincidentally, 0.40mm was the size chosen as a compromise. 8 stations a few hundred meters offshore average a size of 0.41mm, while the five closest to shore are finer at 0.24m.

3.3.2.4 Lateral Boundary Conditions

Originally the long-term values from the Massachusetts Shoreline Change Project were used for boundary change rates, then estimates from eyeballing Google Earth images as seen in Table 7. Finally, the short-term rates from the past few decades were found in the Change Project data. The right/west rate of -0.00255m/day comes straight from that, though the left/east rate of -0.0238m/day was increased slightly to -0.023m/day to bring it more in line with what the Google Earth images showed for 2001-2005 period. During later simulations, the thesis author briefly trialed small positive rates of left 0.0255m/day and right 0.00098m/day to account for a period of accretion after the initial calibration, but it did not produce the desired effect of significantly reducing the inaccurately predicted massive reduction of Wasque Point in the model.

	Date of Google Earth Image	Distance North of 2000 shoreline (m)	Change rate per day
Wasque/Left	12/31/2000	42.4	
	7/6/2003	34.3	-0.00883
	12/31/2003	30	-0.02416
	7/2/2006	39.25	0.01012
	6/26/2011	-77.56	-0.06418
Katama/Right	12/31/2000	18.75	
	2/3/2004	10.44	-0.00736
	7/2/2006	19.62	0.01043
	6/26/2011	-55.73	-0.04140

Table 7. Google Earth Data for Selecting Boundary Change Rate.

CHAPTER 4. GENESIS-T RESULTS

4.1 Model Calibration

The GENESIS-T model was calibrated with over 81 different settings permutations checked, largely analyzing the time period between January 1st, 2002 and March 31st, 2005. The time period was picked as January 1st, 2002 was the earliest averaged wave data available after the gap-filled readings of 2001 were removed. The initial shoreline file was from March 2000, the nearest Google Earth image was from December 2000, and there was another pre-storm Google Earth image for reference from March 31st 2005.

By examining the bathymetry/topography data against the tidal ranges of the area, two east-west points were picked with steep slopes that would have a small uncertainty for estimating erosion/accretion from other Google Earth images of unknown time of day. x=1160 was expected to retreat about 27.3 meters by March 31st, 2005; x=3450 was expected to retreat between 6.3 and 28.3 meters, averaged to 17.3m (x=3440 and x=3460 replaced x=3450 when the model changed from 10x10m to 20x20m).

Table 8. Examples from Calibration Journal (Adjusted for Clarity).

Variable Modified		k_1=0.5, k_2=0.25		
	Test Point	**(Final - Initial) Location (m)**	**Expected Change (m)**	**Absolute Difference (m)**
	1160	-23.092682	-27.3	4.207318
	1420	-0.957336	-60	59.042664
	1440	-1.33255	-60	58.66745
	3440	-26.799316	-17.3	9.499316
	3460	-32.250305	-17.3	14.950305
Variable Modified		k_1=0.65, k_2=0.32		
	1160	-33.812469	-27.3	6.512469
	1420	-11.273468	-60	48.726532
	1440	-11.582428	-60	48.417572
	3440	-28.115814	-17.3	10.815814
	3460	-33.523407	-17.3	16.223407
Variable Modified		same k values, but 5.6m depth of closure		
	1160	-36.814453	-27.3	9.514453
	1420	-14.167725	-60	45.832275
	1440	-14.458466	-60	45.541534
	3440	-28.872375	-17.3	11.572375
	3460	-34.263245	-17.3	16.963245

Given the larger range for the second point, another calibration point seemed wise. By the eastern shore, there was a large arc that formed between the 2000 MHW shoreline and the December 2000 shoreline, which in the center showed about 60m of erosion and seemed a large feature to miss. Thus, x=1420 and x=1440 were added additional calibration points, though x=1440 was later dropped when it failed to reveal any sought pattern x=1420 did not show. However, while multiple permutations matched or approached the other two

points, x=1420's behavior was never properly projected, barely eroding or even accreting in models. Later Google Earth images may somewhat explain the variation: the arc largely appeared over the course of the year 2000 and remained mostly stable in the calibration period, even accreting at times.

Grain size, berm height, depth of closure, and boundary conditions were also varied, but to minimal effect. Initially, the time step was kept at 6 hours. However, when the effects of narrowing the time step to remove the instability warning were explored, there was a troubling discovery.

Model stability error messages occur when the Courant-Friedrichs-Lewy number, or Courant number is greater than or equal to 0.5. Equations 10, 11, and 12 below describe it.

$$R_s = \frac{1(\mathcal{E}_1 + \mathcal{E}_1)\Delta t}{(\Delta x)^2} \tag{10}$$

$$\varepsilon_1 = \frac{2H_b C_{gb} a_1}{(D_B + D_C)} \tag{11}$$

$$\varepsilon_2 = \frac{H_b^2 C_{gb} a_2 \sin \alpha_b}{(D_B + D_C)} \frac{\partial H_b}{\partial x} \tag{12}$$

Where:

H_b is breaking wave height.

C_{gb} is wave group velocity at breaking

α_b is breaking wave angle

(D_B+D_c) is vertical distance between the berm and depth of closure

The source material on this matter guides GenCade, which is based on GENESIS. (Recommendations and Requirements for GenCade Simulations). In simplified terms, simulating a wave yields a less trustworthy answer if the velocity is higher relative to the distance travelled, and it is more trustworthy the smaller the time step is.

Despite stability error messages, varying the time step until the error disappeared yielded little meaningful output difference in GENESIS proper. After the switch to GENESIS-T, the 6-hour time step results were compared to progressively smaller time steps until 0.0625 hours: the average increase in accretion with a smaller time step simulated over 3.25 years was 60 meters, with one point 154 meters further out in the more stable projection.

Although the stability messages became sparse once the time step reached 0.0625, a roughly 25x increase in simulation time required switching from a 10x10m grid to a 20x20m grid. Given the breach was over 100m wide in all Google Earth photos, this was perfectly acceptable. The time step still had to remain 0.0625 hours at this resolution to prevent or sharply reduce the number of error messages (simulations beyond 3.25 years had a small number of stability warnings that did not affects results more than a few meters).

The output differences between using the averaged wave data and the wave data adjusted to Table 6's band limits were negligible at 0.5m and 0.1m on average respectively for GENESIS and GENESIS-T, with a standard deviation of 1.3 and 3 meters.

"Regional contour trend computed from initial shoreline" was an alluring setting after seeing countless models remove 100 unexpected meters from Wasque Point; however, the setting produced wildly inaccurate answers through the rest of the model.

Only k_1 and k_2 remained to adjust. k_1 is the primary calibration parameter and is proportional to the longshore sand transport rate, while k_2 is secondary and is proportional to the wave height gradient along the shore (Di Bona, 2013).

After testing multiple combinations, both from those suggested by literature over the past fifty years and pure numerical exploration. k_1=1 and k_2=0.8 was the most accurate. Originally the three calibration points were not equally weighted in their contribution to the most accurate model, but when the top five models were compared without the weighting, the k_1=1 k_2=.08 model was the still the most accurate.

4.2 Final Bare Shore Model

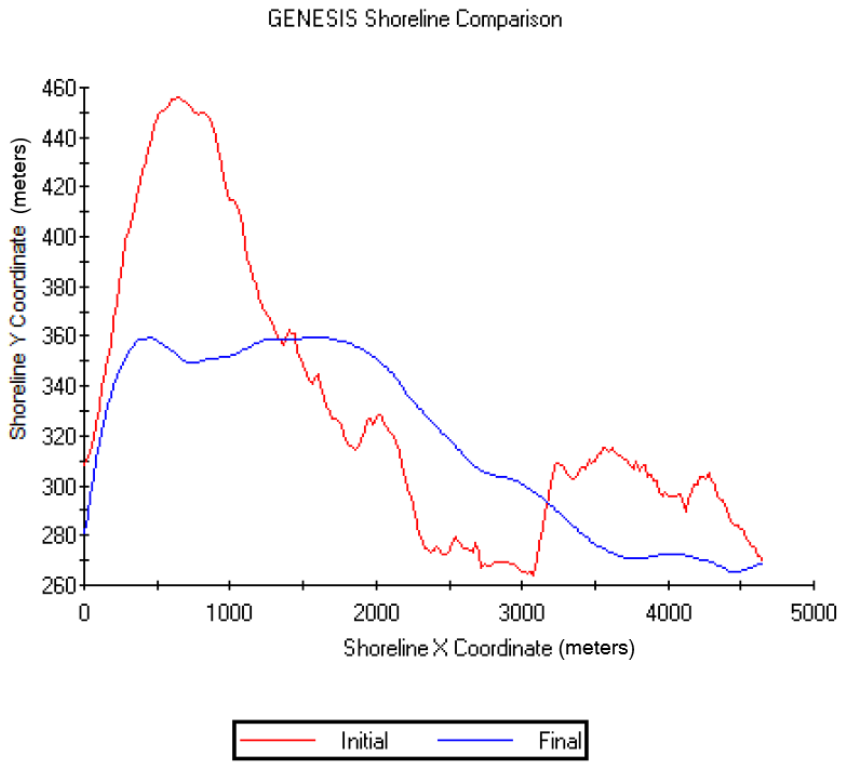

Figure 13. Initial and Final Comparison Between 2002 and 2005, k_1=1 and k_{20}=.8, 20x20m Grid.

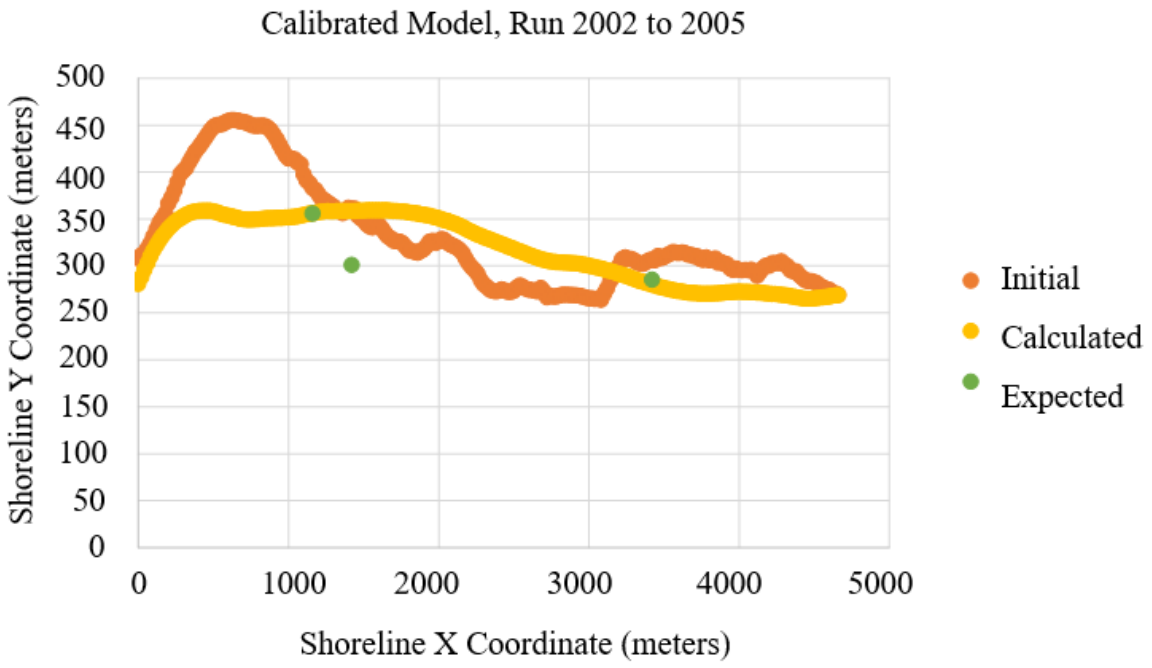

Figure 14. Calibrated Model Run with Calibration Points in Green.

Although Figure 14 shows two of the calibration points fitting quite well with the model, there are multiple important differences that appear when looking at satellite images. The leftmost protrusion on the left which represents Wasque Point actually shrank less than 10m during this time period, and in some places slightly accreted. At x=1340 to 3160 we see accretion; while 5-10 meters of accretion is possibly visible in some Google Earth images, there is nothing like the observed average 36m of accretion for a 1400-meter length of beach.

Going further in time, this model was advanced until April 20, 2007, right after the breach would appear. There was no sign of a breach: except for a maximum of about 10m of erosion in the first 2500 meters of shoreline, there was almost no difference from the 2004

calculation. Despite the very small time step, the stability warning also appeared. However, it was only 0.5755551 (against a cutoff for appearing of 0.5), which during calibration only resulted in differences of a few meters, so the results were accepted.

Going further to April 3, 2014, to see if the breach would heal a year earlier than it did in real life, we see no notable changes outside the trend of Wasque Point levelling out. The stability parameter remained at 0.575551.

Although the calibration also checked April 3, 2015, to see if the breach would heal in real life, as well as September 4, 2018, the end of our wave data and near the last Google Earth image on October 5, 2018, the non-calculated breach obviously did not reappear, the model continued its inexorable quest to become a straight line, and the calibration phase was ended to begin testing breakwaters simplified breakwaters within the model.

4.3 Model with Breakwater(s)

One of the first things noticed during breakwater testing was that processing time increased drastically; the time step was increased from 0.0625 hours to 0.5 before settling at 0.3; once the initial selections were made, the last choices would be verified at 0.0625.

As seen composited in Figure 15, five distances were selected from the coast: 400, 900, 1500, 1800, and 2700m; these distances are from y=290, which is between the end of the main shore and Wasque Point. These distances were chosen based on the location of the depth of closure; multiples of this serve as coastal engineering guidelines which group detached breakwaters into different names depending on distance: offshore, coastal, and beach types of detached breakwaters (Mangor, Drønen, Kristensen, & Kaergaard, 2017).

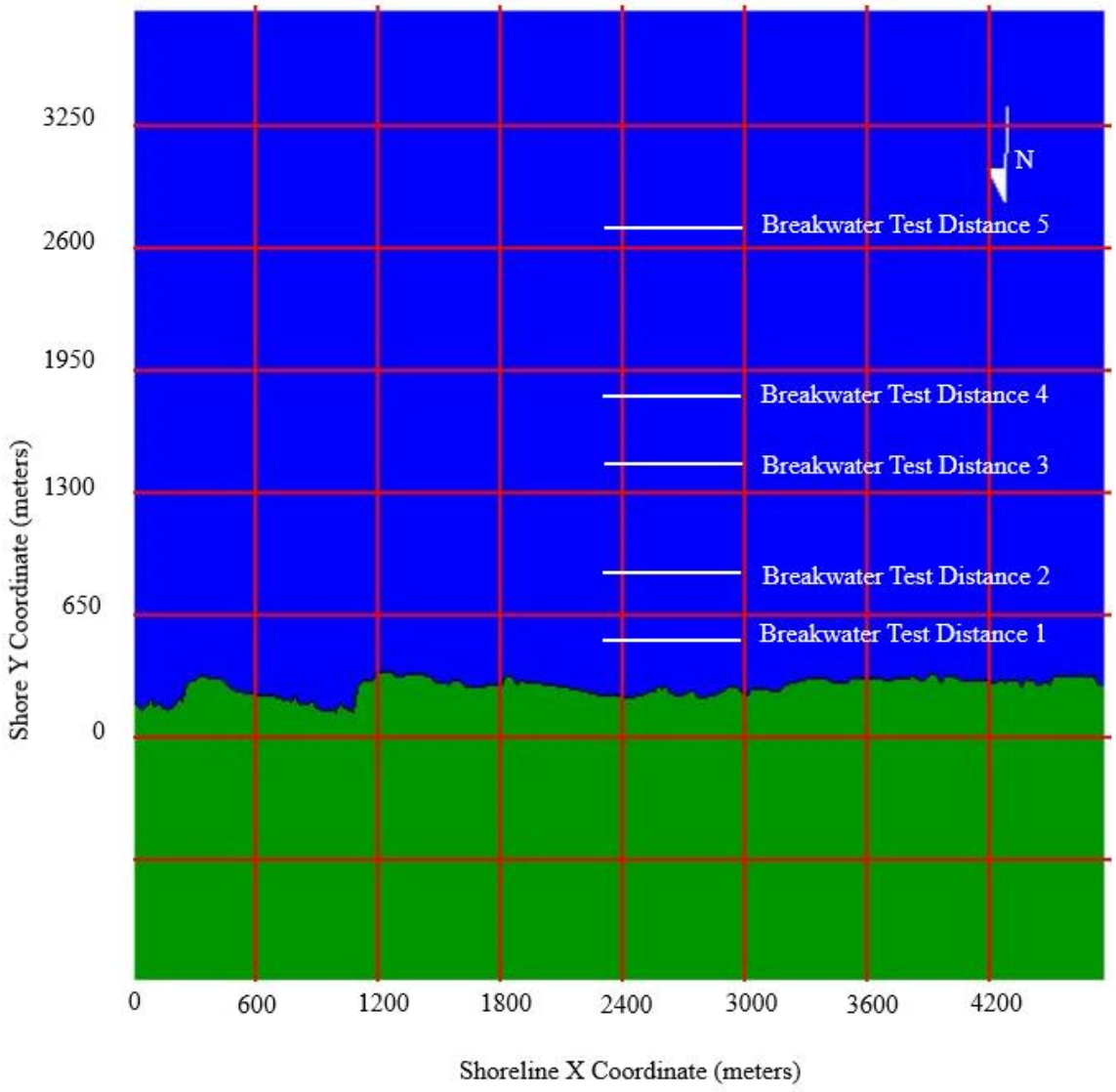

Figure 15. Simplified Detached Breakwaters Distances in GENESIS-T Simulation, Model B Shoreline.

Unfortunately, none of these distances provided the middle ground of accretion without tombolos. Multiple lengths were tested, but the output was either as Figure 16, with half the beach saved and the rest destroyed, or with the breakwater demonstrating little to no effect.

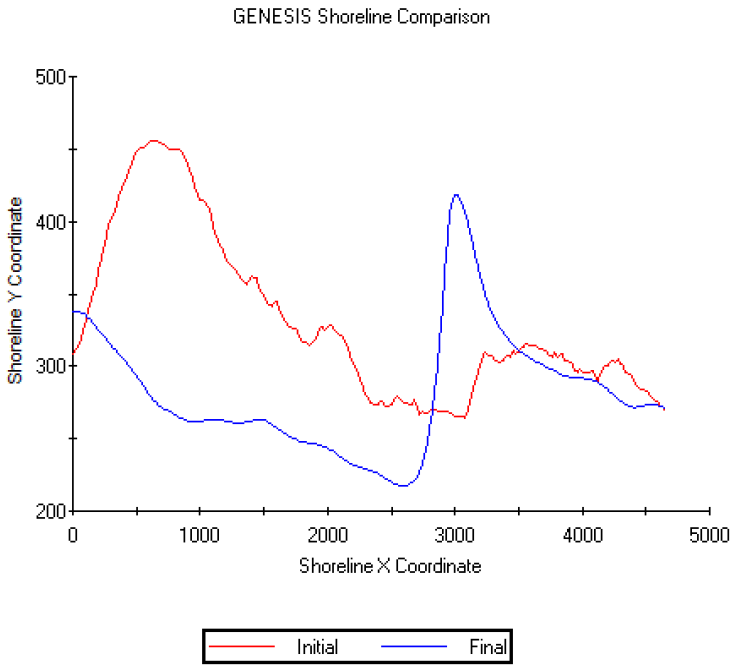

Figure 16. Tombolo Formation in GENESIS T from 300m-Long Breakwater 400m From Shore.

Multiple lengths were tested, but when the distance was great enough to prevent tombolos, any accretion on the thin NP Beach was minimal or negative.

The inability for the thesis author to base a recommendation on the testing, even while further adjusting angle, number of breakwaters, length of breakwater(s), porosity, and breakwater depth largely comes from the problematic Wasque Point: the model predicted that without a breakwater that the area would lose a hundred meters, and with almost any breakwater permutation present, it now loses double that amount.

Later in the conclusion, this tombolo formation from a permanent breakwater will be used to justify a floating breakwater which could be removed seasonally, well before any salients have a chance to become tombolos.

4.4 Reasons for Inadequacy of Model Results

Unacceptable model results generally fall under user error, bad input, and/or problems with the model itself. Below are evaluations of possible sources of error in the hopes that they later guide better models and output

4.4.1 Violation of GENESIS model guidelines

Many of the caveats mentioned in the Army Corps user's manual are violated by applying the GENESIS model to NP Beach. "Beach change inside inlets or in areas dominated by tidal flow" is not modelled well; the change inside the drifting inlet must be modelled if it's going to be modelled closing, and the formerly wave-dominated area became more exposed to the tidal flow that maintained the inlet for years.

"storm-induced beach erosion in which cross-shore sediment transport processes are dominant" are not covered; Dunlop's earlier claims include a winter of storms thinning the beach, which makes violation of this guideline very likely.

Finally, GENESIS is meant to demonstrate long-term changes that follow one particular pattern. In the introduction, the Massachusetts area is noted for cyclical periods of accretion and erosion, and the arc carved into NP Beach between 2000 and 2001 which later filled in is a small-scale example of this.

The violation of these guidelines is likely the strongest contribution to undesirable to model results.

4.4.2 Katama Bay

GENESIS only models the Atlantic Ocean-side shore, while Dunlop noted that the surge of water over the entire width of the beach started from the Katama Bay side. While this is also an inherent weakness of the model, it does not explain why the beach wasn't properly modelled before the breach. If more frequent topographic surveys revealed the surging bay managed to complicate local sediment transports by stealing sediment from the beach berm, it would, but there is currently no evidence for this.

4.4.3 Fast and Variable Shoreline Change

> "Scientists say the mile-long Atlantic coastline of Chappaquiddick stands out as an extraordinary case study in erosion. "If there's another place in Massachusetts that's eroding faster than this one, I can't think of it," said Greg Berman, a coastal processes specialist at the Woods Hole Sea Grant and Cape Cod Cooperative Extension." (Dunlop, As Breach Retreats, Erosion Picks Up Speed, 2013).

By the Massachusetts Shoreline Change Browser data, boundary parts of Wasque point have short term (approximately 30-year) erosion rates of 6.4-7.6 m/year, even if the long term (approximately 150-year) rates are about 1.8-3 m/year. For NP Beach proper, the short-term rates reach as high as 32.3 m/year, even with the long-term rate at 5.5 m/year (Massachusetts Shoreline Change Browser, n.d.). If the magnitude was not a problem for prediction, uncertainty would be. Uncertainty for Wasque Point can be 75.3 m/year, and for NP Beach proper 81.4 m/year.

The rate of erosion may increase the time needed for calibration, as small differences are amplified, but the erosion rate by itself is unlikely the cause of the problems.

4.4.4 Poor Shoreline Input

The traced 2000 MHW shoreline was the only highly accurate shoreline, and yet there cannot lack repercussions for imposing it on 2013 bathymetry and topography. Di Sona's GENESIS preparation noted software available from SMS that can smoothly interpolate shorelines in with bathymetric/topographic data, but this was unavailable to the thesis author. This is compounded by beginning the simulation in 2002. Although there are few differences between the 2000 and the Google Earth images for the years around it, and with the wave data present the changes may only have occurred earlier in the simulated timeline, this was not the case.

Model B simulations disprove this as a major cause of error, though it would likely appear as the first issue using new modelling software suitable to the region. Model B simulations starting in 2013 were also highly inaccurate even though it was built with bathymetry, topography, a shoreline, and wave data all sourced from the same time period.

4.4.5 Distance from MVCO Node and Muskeget Channel Proximity

The wave sensor is located at 41°19.500'N, 70°34.0'W (WHOI, 2020), about 10 kilometers west of the model's initial point. While there are no nearby interruptions above sea level to the normally SSE to SSW-sourced waves, there are extensive and variable shoals south of the eastern half of Norton Point beach. So close to the Muskeget Channel, where currents could interact with the true waves hitting Norton Point Beach, this interaction could also justify reversing patterns of accretion and erosion seen on Google Earth images of the area. If the occasional sight of accretion instead of erosion in these images was not just caused by variations in satellite image capture time between MHW and MLW, weakened/varying

waves combined with non-modelled current influences would be another cause of model corruption.

This is likely a minor source of inaccuracy for NP beach proper, though Wasque Point is likely strongly affected by Muskeget Channel. However, the channel likely had nothing to do with the breach, so it not a source for error for predicting breach formation.

CHAPTER 5. NON-MODEL BREACH FACTOR EVALUATION

Both concurrent with GENESIS-T model development and after it failed to predict the breach, the thesis author hoped that wave action alone could predict it. It did not, nor did looking at the rising sea levels or tides alone in the area. Tom Dunlop, a writer and local in the area, places the breach down to four simultaneous factors. Unfortunately, there is not enough historical wave and tidal data to quantify these factors into a predictive model, but they do correspond with previous observational of another major breach, the 1953/1954 described by Ogden in Table 1.

5.1 Wave Action Alone

The initial hypothesis was that intensive wave action alone was responsible for the breach, and likely previous breaches in NP Beach. Average intense wave action could slowly weaken the beach until it breached, particularly intense wave action during a storm could tear open the beach, and either types of wave action after a breach could maintain or widen the breach.

This hypothesis was invalidated by several pieces of data, presented in achronological order.

"In the early 1970s the Army Corps of Engineers proposed building a ten-foot high berm south of South Beach to block storm waves from washing over Norton Point and breaking it open. But Ogden's report of 1974 showed that it was the beach failing from Katama Bay outward – not a rushing in of water from the sea – that caused Norton Point to give way. This may be why he added an eyewitness account that stressed the water driving outward from the bay to the sea. The Army Corps of Engineers soon abandoned the idea of building a berm south of South Beach. " (Dunlop, REVISED: A HISTORY OF THE OPENINGS (AND CLOSINGS), 2014)

Thus, intense wave action from the south has never been seen by eyewitness accounts as the striking blow to open the beach.

While the wave height histograms in Figure 6 show 2008 as the most intense year, it also shows several years including 2007 having a notable number of wave heights above 2.5m.

When calculating depth of closure, the peak significant wave heights in the raw, along with top 36 readings per year (see Table 9 below)**,** were recorded**.** 2007 was the first year chronologically to be in the top 8, but it is barely above 2006 which did not have a breach. 2015, 2016, and 2018 all had minor breaches but were weaker in terms of 12-hour period, and 2017 was the strongest but had no breach. The most powerful 2008 season can be excused as maintaining the breach longer, but there is no other evidence for or against this theory. In short, wave heights alone cannot predict the breaches.

Table 9. Depth of Closure Calculation/Highest Wave Data.

	2001	**2002**	**2003**	**2004**	**2005**	**2006**	**2007**	**2008**	**2009**
Highest Wave Per Year, Meters	2.2	3.9	4.1	3.6	4.6	4.7	4.7	11.3	4.8
Wave Only Surpassed 12 Hours Per Year, Meters	1.9	3.2	3.5	3	3.5	4.1	4.1	5.1	3.7
	2010	**2011**	**2012**	**2013**	**2014**	**2015**	**2016**	**2017**	**2018**
Highest Wave Per Year, Meters	4.6	5.2	4.8	5.3	4.4	4.3	4.5	5.1	4.1
Wave Only Surpassed 12 Hours Per Year, Meters	3.8	3.9	3.9	4.2	3.9	3	4	3.9	3.5

5.2 Rising Seas

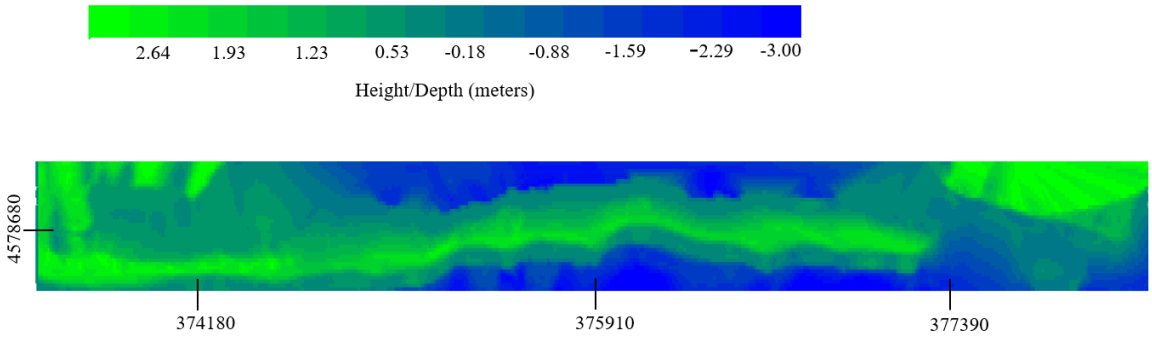

Figure 17. Topography of Norton Point Beach, UTM, 2013.

In the 2013 topography see in Figure 17, although some of the east wing has NAVD heights above 3m (MSL is -14.5cm NAVD88), and just left of the breach area is a little over 2 meters, even the newly rebuilt center often has a peak between 1.8 and 2m. Going by the local Nantucket sea level projections (NOAA, 2020), sea level rise was 8.3mm/year between September 2001 and January 2015, and 17.3mm/year between March 2015 and December 2019. High compared to global mean sea level rise (2.8 to 3.6mm/year) (Church & Clark, 2013), it still by itself cannot have caused the breaches in the past, nor is it likely to cause them in the next 50 years. The NOAA Sea Level Rise Viewer, which appears to use roughly the same date for topography as used in the GENESIS model, does not show a new cross-beach water covering until MHHW is 1.5m elevated, most of the beach is covered at 2.1m, and all but a few specks are submerged at 3m (NOAA, 2019).

As far as Dunlop's premise that a series of winter storms had shrunk the beach and made it vulnerable to breaching, there is insufficient data. By the Beaufort scale (which ranks wind

speed by observed sea states and has “storm” defined by 89-102km/h winds and/or 9-12.5m wave heights) (Britannica, 2017), the island almost never has storms as seen by wind speed or wave height. This leaves storm surge as the primary cause of breaches.

5.3 Examining the Four Breach Influences Noted by Dunlop

5.3.1 Great Storm

For the first claim of previous storms, there is no concise definition of “storm” beyond the Beaufort scale, which was never met. The top 10% of significant wave height in the MVCO data for 2007 was 2m and above, which was surpassed starting on April 10th on 94 20-minute occasions before 1200 UTC on the 16th and 75 more occasions before 1320 UTC, after the breach and when the waves started to consistently return to normal. For comparison, the averaged wave data had 1.7m for the top 10% and a mean of 1.0m.

5.3.2 Damaged Beach

For the second claim on the condition of the beach, no confirmed measurements of the beach were found, other than that LANDSAT imagery confirms the beach was intact right.

Table 10. Winter Average Significant Wave Heights, Meters.

Winter Beginning	Oct-March Average SWH	Standard Deviation	Dec-March Average SWH	Standard Deviation
2001	1.13	0.496	1.19	0.496
2002	1.14	0.616	1.15	0.602
2003	1.14	0.618	1.17	0.601
2004	1.03	0.544	1.08	0.528
2005	1.21	0.607	**1.20**	0.578
2006	**1.26**	0.666	**1.36**	0.637
2007	1.21	0.711	1.31	0.770
2008	**1.27**	0.690	**1.34**	0.659
2009	1.08	0.605	1.13	0.642
2010	1.11	0.605	1.10	0.604
2011	1.08	0.584	1.11	0.630
2012	1.09	0.609	1.11	0.621
2013	1.18	0.669	1.24	0.661
2014	1.09	0.563	1.10	0.568
2015	1.22	0.593	1.29	0.621
2016	1.11	0.449	1.20	0.382
2017	1.20	0.619	1.24	0.588

Looking at Table 10, the 2006-2007 winter was indeed the most powerful winter by average wave-height (absolutely looking at December to March and with one-decimal-point significant figures October to March).

Table 11. Wave Energy Per Unit Area of the Top 36 20-Minute Significant Wave Heights, by Year, Joules Per Square Meter. Italicized years are within one standard deviation of the median.

Year	J/m^2
2008	2700598
2017	*956774*
2013	*946679*
2011	*865917*
2012	*840704*
2007	*831764*
2006	*826967*
2016	*800587*
2014	*766785*
2010	*713120*
2009	*711337*
2005	*677636*
2018	*649271*
2003	*611402*

Looking at Table 11, 2006 and 2007 were among the most energetic years of the 2000s; the wave energy density is calculated with the below Equation 13 (NIWA, 2004).

$$E_{Top\ 36} = \sum_{n=1}^{36} \frac{1}{8} \rho g H_n^2 \tag{33}$$

5.3.3 Exceptionally High Tide

Leading into the third claim, that there was a particularly high tide on the evening of April 16th-17, let's first look at the PAROS tide data to see if the winter was also intense as far as sea surface height/storm surge. There was a new moon on April 17th, which would intensify the tidal range (Moon Phases Calendar, n.d.). There is a clear elevation above the neighboring days in Figure 18 and in the nearby Nantucket data in Figure 19.

The Nantucket data also displays the prediction for the date, showing the effects of possible atmospheric forcing from the storm, causing the seas to arrive above expected tide levels.

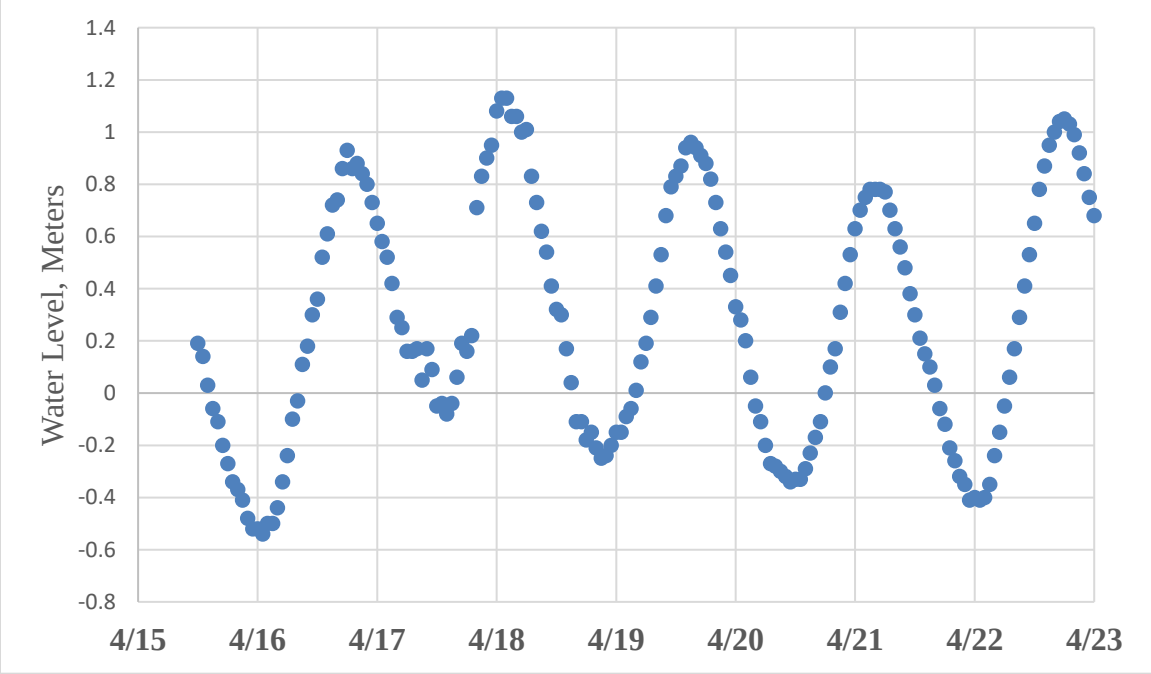

Figure 18. PAROS Water Level Data, 4/15 to 4/23/2007

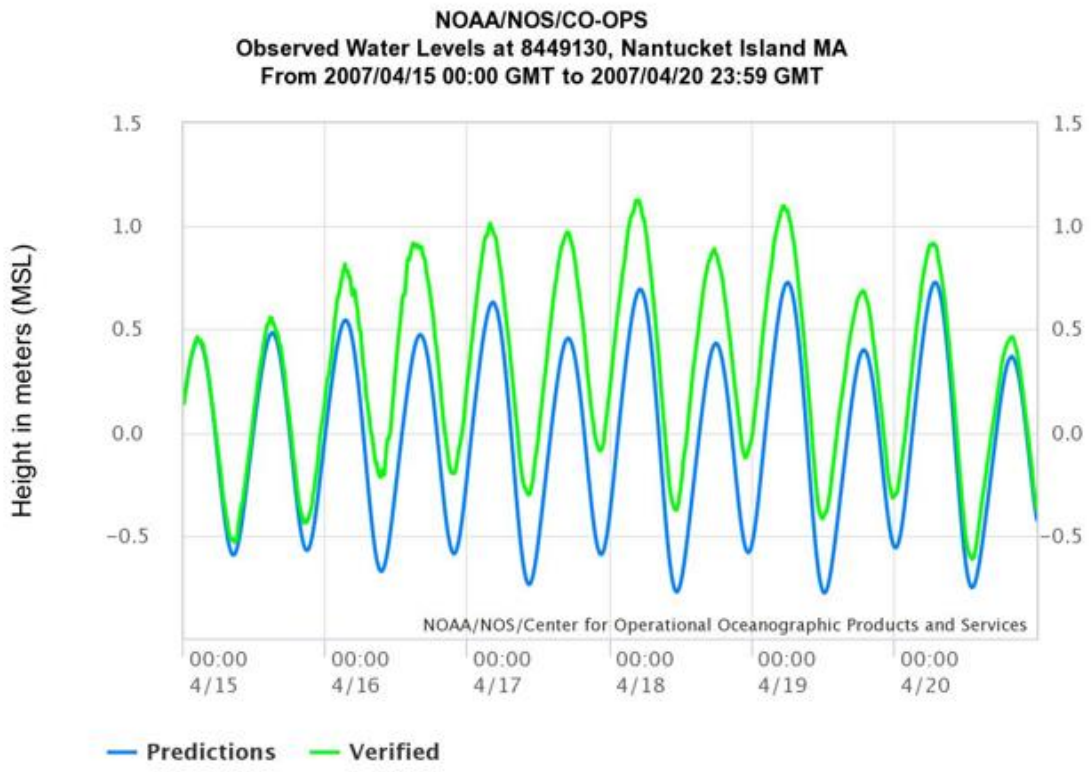

Figure 19. Nantucket NOAA Tide Gauge Data 4/15 to 4/20/2007

There are no results in the literature review between July 1, 2001 to April 1, 2007 for "'overwash' 'Norton Point'", but there are several for following dates describing the breach. A 2013 overwash study of neighboring beaches does not note any local overwash events after 1997 (Carruthers, Lane, Evans, Donnelly, & Ashton, 2013). Similar high tides may also be associated with breaches.

5.3.4 Wind and Combined Factors

With the final claim "The wind veered to northwest as the tide fell in the Atlantic just before midnight on April 17. But the water in the bay remained exceptionally high", the

effect cannot be confirmed, but the MVCO database does have meteorological data: winds were blowing to the northwest for all of the 16th and on the 17th until 2:20 UTC, when they were blowing firmly from the west as seen in Figure 20. This conflicts with the claims, but they could be from a different anemometer.

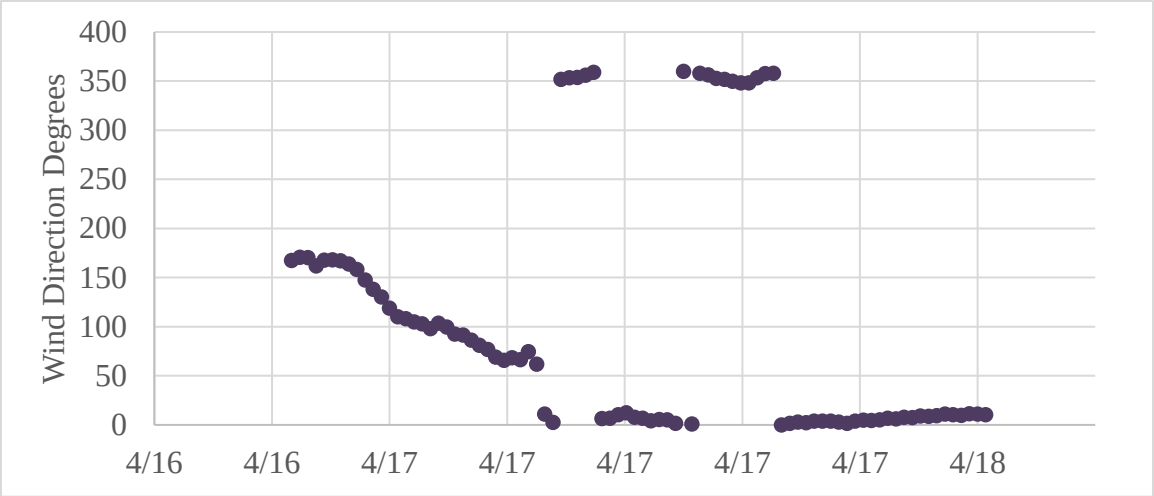

Figure 20. MVCO Wind Data 4/16 to 4/18/2020. 180 Degrees is from the South.

CHAPTER 6. SPECIFIC-STYLE BREAKWATER SOLUTIONS

6.1 Background

Despite the inability to accurately model the beach's behavior with or without a breach or breakwater, below the thesis author provides the following data for future scientists and engineers who may justify one. The existing coastal structures of the area, the area construction supplies, and basic breakwater armor calculations may hasten the design process.

6.1.1 Existing Structures near Norton Point Beach

An engineering survey of Edgartown published in 2009 noted no known breakwaters, though there were 3 bulkheads/seawalls, 2 revetments, and one groin/jetty. The survey unfortunately did not note their materials more specifically than stone, stone with concrete mortar, wood, and steel. "compacted washed stone fill" is mentioned in several plans for building, but it does not name a size or source (Bourne Consulting Engineering, 2009). It is important to note that the breakwater proposed in this paper would be legally prohibited, as since 1980, Executive Order 101 has forbidden the construction of hard engineering structures on barrier beaches except to maintain navigation channels (EXECUTIVE ORDER No. 181: Barrier Beaches, 1980).

6.1.2 Area Construction Supplies

Massachusetts was once famous for supplying granite (Brayley, 1913), and limestone is also available in quantity (Dale, 1923). For the purposes of calculation, the density of

Massachusetts' granite is 2.662kg/m^3, and the density of Massachusetts limestone is 2.643 kg/m^3 (The M.W. Kellogg Company, 1972; Dale, The Chief Commerical Granites of Massachusetts, New Hampshire, and Rhode Island, 1908). The derived specific gravity of granite is 2.662, and the specific gravity of limestone is 2.64. On the island proper, there are no quarries for granite or other sizable rocks, although clay and sand were previously extracted (Baer, 2016). Thus, all rock for construction will need to be shipped in from the mainland.

There is no modern record of marine-targeted shaped concrete manufacturers in Massachusetts, although there are multiple general handlers of precast concrete operations.

6.2 Factors for Multiple Designs

6.2.1 Visibility

If a permanent breakwater, such as a rubble mound or vertical breakwater, were recommended for the region, local opposition to visible offshore construction has been strong (Asimow, 2019). Submerged rubble mound breakwaters step around this problem by disappearing beneath the sea after construction. However, these are best in situations where a higher degree of wave transmission is allowed because of existing vegetative or other defenses, and the slender beaches of Martha's Vineyard possess few of these (Seabrook & Hall, 1998). There are conjectures on tide-adapting submerged breakwaters: though the area is microtidal, the model could be useful if the same structures could be adapted to the occasional large storm surges (Lee, Jeong, & Hur, 2019).

6.2.2 Slope

The flatter the slope, the greater stability of the breakwater (Guler, Ergin, & Ozyurt Tarakcioglu, 2014) (Waterways Experiment Station, 1953). However, for a structure of set height, the amount of material necessarily increases with height (thus why vertical breakwaters are desirable in particularly deep waters). For re-shaping/dynamic breakwaters, a sleep stope may exist in the beginning, and material is allowed to move without drastic damage to the structure. The original Van der Meer test slopes between 1:1.5 to 1:6 will be used below (Eldrup, Lykke Andersen, & Burcharth, 2019).

6.2.3 Armor Size Calculations

The outer layer of most rubble mound and some composite breakwaters is armor: larger stones or shaped concrete that absorb most of the incoming wave energy. The right shape, size, and placement is important to prevent damage to the armor and/or the other parts of the breakwater.

6.2.3.1 Hudson's Equation

Hudson's equation allows estimating the median weight per armor block for rubble breakwaters (New York State Department of Environmental Conservation).

$$W = \frac{\gamma H^3}{K_D \Delta^3 \cot(\theta)} \tag{14}$$

γ is the specific weight of the armor unit (density*9.8 m/s^2).

H is the design wave height; here are tested the top significant wave height of 2001-2019 (11.3m) and H_{10} (1.7m). Although generally a probabilistic approach based on a wave expected within the lifespan of the breakwater would be preferable, this has been omitted as by the time of writing, the decision was made to support an intermittent floating breakwater without a standard timeline (being deployed seasonally).

K_D is an empirical value based on physical testing: here is used 3.5 for breaking wave with rough quarried stone and 10 for dolos and other shaped concrete structures (Allen, 1998).

Δ is the dimensionless relative buoyant density of rock ([specific gravity – 1], 1.37 for concrete (Weight Per Cubic Foot And Specific Gravity (Typical), 2020), 1.64 for limestone, and 1.66 for granite).

θ is the slope of the breakwater.

Table 12. Concrete Median Weight and Mass.

				Highest Wave (11.3m)		H10 (1.7m)	
γ	Δ	K_D	cot(θ)	Weight (N)	Mass (kg)	Weight (N)	Mass (kg)
2.37	1.37	10	1.5	870	89	3	0.3
			2	650	66	2.2	0.23
			3	430	44	1.5	0.15
			4	330	34	1.1	0.11
			5	260	27	0.9	0.09
			6	220	22	0.7	0.08

Table 13. Granite Median Weight and Mass.

				Highest Wave (11.3m)		H10 (1.7m)	
γ	Δ	K_D	cot(θ)	Weight (N)	Mass (kg)	Weight (N)	Mass (kg)
2.64	1.64	3.5	1.5	1600	164	5.5	0.56
			2	1210	123	4.1	0.42
			3	810	82	2.7	0.28
			4	610	62	2.1	0.21
			5	300	49	1.6	0.17
			6	250	41	1.4	0.14

In Table 13, the granite masses are roughly twice as heavy as their shaped concrete counterparts in Table 11. Comparing Tables 13 and 14, there is no meaningful difference in the necessary sizes/weights between the two rock types. However, granite has a long history of use in marine environments and is more resistant to ocean acidification.

Table 14. Limestone Median Weight and Mass.

				Highest Wave (11.3m)		**H10 (1.7m)**	
γ	Δ	K_D	cot(θ)	Weight (N)	Mass (kg)	Weight (N)	Mass (kg)
2.66	1.66	3.5	1.5	1570	160	5.3	0.54
			2	1180	120	4	0.41
			3	780	80	2.7	0.27
			4	590	60	2	0.2
			5	470	48	1.6	0.16
			6	400	40	1.3	0.14

6.2.3.2 Van der Meer's Formula

Before using the Van der Meer equation for a different perspective on which blocks are best to use, it is necessary to calculate the Iribarren number, also known as the surf similarity parameter, which describes how a wave will break on a particular slope (Hedges, n.d.).

$$\xi = \frac{tan\ (\theta)}{\sqrt{H/L}} \tag{15}$$

With $L=1.56T^2$ as the wavelength, yielding waves of 56m and 1577m for the significant wave (1m high and 6 seconds) and the highest wave (11.3m and 31.8 seconds), a notional permeability *P* of 0.4, and plunging and surging coefficients based on irregular rocks of C_{pl}=5.96 and C_s=1.16 (Guler, Ergin, & Ozyurt Tarakcioglu, 2014), it is now possible to calculate the critical Iribarren number for a particular structure of a particular slope, independent of any specific wave, using Equation 16.

$$\xi_{crit} = \left(\frac{C_{pl}}{C_s} P^{0.31} \sqrt{\tan\ (\theta)}\right)^{\frac{1}{P+0.5}} \tag{16}$$

Table 15. Iribarren Numbers for Various Slopes.

cot(θ)	ξ,11.3m	ξ,1.0m	ξcrit
1.5	7.9	5.0	3.6
2.0	5.9	3.8	3.0
3.0	3.9	2.5	2.4
4.0	3.0	1.9	2.1
5.0	2.4	1.5	1.8
6.0	2.0	1.3	1.7

Combined with the Guler's form of the Van der Meer (Equations 17 and 18), which are chosen based on the above Iribarren numbers, a damage parameter S_d of 2 and N=8500 waves (the maximum number of waves recommended by Van der Meer), now presented are two pre-prototype projections for riprap size (Van der Meer, 1988). After first running the calculations for granite and seeing unrealizable (>4m) diameters for the maximum wave seen, $H_{2\%}$ of 3m and 7.7 seconds is added for the convenience of the designer using Equations 19 and 20, which Van der Meer specifically created for $H_{2\%}$.

Plunging waves: $\xi < \xi_{crit}$:

$$\frac{H_S}{\Delta \mathrm{D}_{n50A}} = 6.2P^{0.18}\left(\frac{S_d}{\sqrt{N}}\right)^{0.2}\xi^{-0.5} \tag{17}$$

Surging waves: $\xi \geq \xi_{crit}$:

$$\frac{H_S}{\Delta \mathrm{D}_{n50A}} = P^{-0.13}\left(\frac{S_d}{\sqrt{N}}\right)^{0.2}\sqrt{\cot(\theta)}\,\xi^{P} \tag{18}$$

Plunging $H_{2\%}$ waves: $\xi < \xi_{crit}$:

$$\frac{H_{2\%}}{\Delta \mathrm{D}_{n50A}} = 8.7P^{0.18}\left(\frac{S_d}{\sqrt{N}}\right)^{0.2}\xi^{-0.5} \tag{19}$$

Surging $H_{2\%}$ waves: $\xi \geq \xi_{crit}$:

$$\frac{H_{2\%}}{\Delta \mathrm{D}_{n50A}} = 1.4P^{-0.13}\left(\frac{S_d}{\sqrt{N}}\right)^{0.2}\sqrt{\cot(\theta)}\,\xi^{P} \tag{20}$$

Table 16. Van der Meer Median Block Diameters by Wave Height and Slope, Meters.

cot(θ)	11.3m	1.0m	$H_{2\%}$
1.5	7.7	0.8	2.0
2.0	7.5	0.8	1.5
3.0	7.2	0.8	1.4
4.0	7.0	0.6	1.3
5.0	6.8	0.5	1.2
6.0	6.7	0.5	1.1

6.2.3.3 Comparison

Now to compare outputs, the Hudson-derived masses must be converted with Equation 21 to produce Table 17.

$$D_{n50} = (\frac{M}{\rho})^{1/3} \quad (21)$$

Table 17. Hudson and Van der Meer Diameters, Granite.

	Highest Wave	Highest Wave	$H_{2\%}$ (3m)	$H_{2\%}$ (3m)	H_{10} (1.7m)
	Hudson Diameter (m)	Van der Meer Diameter (m)	Hudson Diameter (m)	Van der Meer Diameter (m)	Hudson Diameter (m)
cot(θ)					
1.5	0.40	7.72	0.09	2.00	0.06
2	0.36	7.50	0.08	1.53	0.05
3	0.31	7.20	0.06	1.37	0.05
4	0.29	7.00	0.06	1.26	0.04
5	0.27	6.84	0.06	1.18	0.04
6	0.25	6.72	0.05	1.13	0.04

The massive difference in the two formulae's results reminds the thesis author that damage to the breakwater cannot always be avoided in in realistic construction. 7m diameter stones would be largely unavailable and difficult to transport, but the $H_{2\%}$ 1.1-2m sizes are in an obtainable yet upper range (Federal Highway Administration, 2006). During a 25- or 30-year lifespan, should the area see the 2008 storm again, a dynamic option where stones or other building materials can be moved is preferable.

Note that despite using these two methods, the Guler comparative study generally recommends a newer modification of the Van der Meer equation known as the Van Gent equation in many situations. However, it does not apply here as $H_{2\%}$ is over 40% more than the significant wave height.

6.3 Rubble Mound Breakwaters

Rubble Mound breakwaters are the most well-known breakwaters, using varying slopes of stone or shaped concrete to modify incoming waves (Takahashi, 2002). With more solid concrete or quarry run centers, these breakwaters will diffract waves more, but other armored or multi-layered rubble mound breakwaters can diffuse while allowing larger amounts of water and sediment to pass through. Adjusting this permeability in the GENESIS-T model to maintain the beach while preventing tombolo formation was unsuccessful.

6.3.1 Berm Breakwaters

6.3.1.1 Dynamic Berm Breakwaters

Technically a type of rubble mound breakwater, the dynamic berm breakwater has a large porous berm at or above still water level and seaward of the rubble mound (Andersen & Burcharth, 2010). Using multiple classes of stone sorted in multiple sizes, which often allows the use of cheaper material from a single quarry, the relatively large size compared to vertical or floating breakwaters would be a disadvantage for any island construction. However, this may be somewhat offset by the ability to use conventional construction contracting equipment, unlike those necessary during the delicate deposition of larger stones/shaped concrete (PIANC, 2003). Dynamic berm breakwaters are appropriate according to PIANC when H_oT_{om} is greater than 70, where

$$\text{Ho} = \frac{H_{1/3}}{\Delta D_{n50}} \tag{20}$$

Whether using $H_{1/3}$, $H_{2\%}$, H_{10}, or any wave criteria other than H_{max} for construction, a dynamic berm breakwater is easily possible with common materials, only needing granite or concrete material between 2cm to 20cm, as seen in Table 18.

Wave Height	Wave Period (s)	Granite (m)	Limestone (m)	Concrete (m)
$H_{max,}$ 11.3m	31.8	3.09	3.75	3.75
H_{10}, 3m	7.7	0.20	0.20	0.20
$H_{2,}$ 1.7	1.6	0.02	0.02	0.02
$H_{1/3}$, 1	6	0.05	0.05	0.05

Table 18. Maximum Dynamic Breakwater Median Rubble Size by Material.

6.3.1.2 Static "Icelandic" Berm Breakwaters

Static berm breakwaters require multiple classes of stone and are designed to have limited movement in their profile over their functional life. Should designers fear another April 2008 storm, existing projects have only really explored design wave heights of 8.0 and 9.2m in Iceland and Norway. 160 minutes of that storm exceeded those thresholds. A tandem breakwater situation could reduce the necessary design wave height for the Icelandic breakwater, but this would further complicate the busy waterways of the region (Sigurdarson, Smarason, Viggosson, & Bjørdal, 2006). If the design were performed around using $H_{1/3}$, $H_{2\%}$, or $H_{10,}$ but not H_{max}, an initially re-shaping but later static berm breakwater could use rocks as small as 2cm or as large as 42cm (see Table 19). These

initially re-shaping varieties are sometimes preferred to fully dynamic berm breakwaters, as there is less risk of damage to riprap during re-shaping.

Wave Height	Wave Period (s)	Granite (m)	Limestone (m)	Concrete (m)
$H_{max,}$ 11.3m	31.8	3.18-5.48	3.14-5.41	3.80-6.56
H_{10}, 3m	7.7	0.20-0.35	0.20-0.35	0.24-0.42
$H_{2,}$ 1.7	1.6	0.02-0.04	0.02-0.04	0.03-.05
$H_{1/3}$, 1	6	0.05-0.09	0.05-0.09	0.06-0.11

Table 19. Range of Median Rubble Sizes for Initially-Reshaping Static Breakwater by Material.

For a fully static breakwater, the median rubble size would need to exceed the largest values in Table 19.

6.4 Vertical Breakwaters

Vertical breakwaters come in several varieties: monolith concrete, caisson, perforated caisson, sloping top-wall caisson, semi-circular caisson, cellular blocks, and block (interlocking) masonry (Takahashi, 2002). They are also sometimes composited with a rubble mound, but this loses their chief advantage in deeper water of using less material per linear meter. As the water off the southern coast of Martha's Vineyard is relatively shallow, this advantage is not necessary. Furthermore, without perforations the diffraction from vertical breakwaters can make navigation difficult.

The repair of a vertical breakwater can require so many different steps that it may be more cost effective to choose and develop a new design. When a 1992 northern Japanese storm exceeded the design wave height of a vertical breakwater, the following flaws appeared:

"1) large scale-scouring in front of the breakwater 2) meandering sliding at the northern end 3) scattering of wave-dissipating concrete blocks and caisson failure at the concaved section due to impulsive breaking pressures 4) scouring underneath the caisson at the southern breakwater head" (Takahashi, 2002).

6.5 Floating Breakwaters

Floating breakwaters come in multiple shapes; some are tethered to the seafloor while others float freely. Their freedom of movement, compared to vertical and rubble mound breakwaters, generally restricts them to areas of low wave height or very deep areas where a continuous structure from seafloor to sea level is untenable (McCartney, 1985).

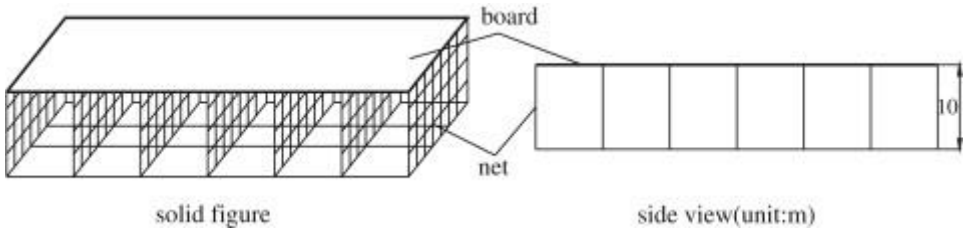

Figure 21. Floating Board-Net Breakwater (Dong, et al., 2008, Used With Permission).

However, advances in board-net (see Figure 21) breakwater design allow the damage of much higher waves to be diminished. With breakwater width/wavelength ratios of 1.2 to

2.8, transmission coefficients with a 4.5-meter wave reach 0.4 to 0.8, and for a 6.0-meter wave as low as between 0.2 to 0.6 (Dong, et al., 2008). Although a thousand-meter breakwater would only demonstrate this against wavelengths up to 825 meters, during the intense winter storm season of 2008, only about 11-17 hours of intense wave activity ($\geq$21 second period and wave heights above 3 or 4 meters) would have been unaddressed. Other advantages will be addressed in the conclusion.

Disadvantages of floating breakwaters are that they can become lost far more easily than permanent breakwater types. Mooring lines break and can be snagged on anchors. The materials for floating breakwaters are almost always more expensive by weight and volume than the stone or concrete used in other types.

CHAPTER 7. CONCLUSION

Although the reliability of the GENESIS-T model in this situation was low, combined with the non-GENESIS analysis and breakwater options, there is a possible solution to reduce the erosion and occasional breaching of Norton Point Beach through the use of temporary floating breakwaters.

There are no realistic ways to reduce the storm surge within Katama Bay, but the preceding winter of intense wave weakened the beach, allowing for the surge to produce such a drastic change. A floating breakwater can reduce wave transmission and leave a stronger beach to endure storm surge. Relatedly, as far as predicting breaches, the only reliable strategy until a better model is developed is to keep an eye on storms that coincide with new or full moons.

The floating board-net breakwater mentioned has multiple advantages. It avoids the local opposition to offshore construction. Similarly, it can avoid being present altogether during the active summer season, only being deployed during the blustery and depopulated winter months. Promoting stronger accretion at the thinnest point at some dates and retreating further south to protect the entire beach area may be feasible.

CHAPTER 8. FUTURE RESEARCH

The first step for future research is an accurate model of Katama Bay, Norton Point Beach, and the nearby Atlanta Ocean. especially the vagaries of growing and shrinking Wasque Point. This would likely begin decoupled from inlet-formation, though not necessarily from inlet closure.

An accurate model for the probability of inlet formation would require more frequent and accurate information on shoreline thickness and shape. As the beach has breached again at least twice in the thin eastern section since 2015, tracking its thickening may be a simple but effective means of predicting when breaches are likely.

Considering that in nearby ponds there are intentional breaches cut periodically, the Martha's Vineyard community would likely not seek to end all inlets, but would likely prefer them to resemble the post-2015 inlets: small and gone within a few months, if not sooner.

The floating breakwater model discussed has been largely tested in water deep enough so that non-floating designs would not be justified. Further testing it in shallow water and the transition from shallow to deep water should occur before deployment.

APPENDIX A: LETTER OF PERMISSION

ELSEVIER LICENSE
TERMS AND CONDITIONS

Aug 13, 2020

This Agreement between Mr. Ian Emerson ("You") and Elsevier ("Elsevier") consists of your license details and the terms and conditions provided by Elsevier and Copyright Clearance Center.

License Number	4887360844214
License date	Aug 13, 2020
Licensed Content Publisher	Elsevier
Licensed Content Publication	Ocean Engineering
Licensed Content Title	Experiments on wave transmission coefficients of floating breakwaters
Licensed Content Author	G.H. Dong,Y.N. Zheng,Y.C. Li,B. Teng,C.T. Guan,D.F. Lin
Licensed Content Date	Jun 1, 2008
Licensed Content Volume	35
Licensed Content Issue	8-9

Licensed Content Pages	8
Start Page	931
End Page	938
Type of Use	reuse in a thesis/dissertation
Portion	figures/tables/illustrations
Number of figures/tables/illustrations	1
Format	electronic
Are you the author of this Elsevier article?	No

https://s100.copyright.com/AppDispatchServlet

8/13/2020 RightsLink Printable License

Will you be translating?	No
Title	EXPLORING THE APPLICABILITY OF DETACHED BREAKWATERS TO PREVENT EPHEMERAL INLETS IN NORTON POINT BEACH, CHAPPAQUIDDICK ISLAND, MA

Institution name	Georgia Institute of Technology
Expected presentation date	Aug 2020
Portions	Figure 3. The board-net floating breakwater.
Requestor Location	Mr. Ian Emerson REDACTED REDACTED United States Attn: Mr. Ian Emerson

REFERENCES

A Fine Load of Codfish. (1878, June 23). *The New York Times*. Retrieved from https://timesmachine.nytimes.com/timesmachine/1878/06/23/80718997.pdf

Allen, R. T. (1998). *Concrete in Coastal Structures*. London. Retrieved from https://babel.hathitrust.org/cgi/pt?id=mdp.39015043145203&view=1up&seq=76&q1=3.5

Andersen, T. L., & Burcharth, H. F. (2010, April). A new formula for front slope recession of berm breakwaters. *Coastal Engineering, 57*(4), 359-374. doi:10.1016/j.coastaleng.2009.10.017

Andrews, B. D., Baldwin, W. E., Sampson, D. W., & Schwab, W. C. (2018, May 2). Continuous bathymetry and elevation models of the Massachusetts coastal zone and continental shelf. doi:https://doi.org/10.5066/F72806T7

Asimow, N. (2019, June 29). Fishermen, Climate Activists Clash Over Wind Farm Cable. *Vineyard Gazette*. Retrieved from https://vineyardgazette.com/news/2019/06/29/fishermen-climate-activists-odds-emotional-hearing-wind-farm-cable

Aubrey, D., & Gaines, A. (1982, October). Rapid formation and degradation of barrier spits in areas with low rates of littoral drift. *Marine Geology, 49*(3-4), 257-277. doi:10.1016/0025-3227(82)90043-3

Baer, C. (2016, September 27). This Was Then: The marble works of Indian Hill. *The Martha's Vineyard Times*. Retrieved from https://www.mvtimes.com/2016/09/27/marble-works-indian-hill/

Bourne Consulting Engineering. (2009). *Massachusetts Coastal Infrastructure Inventory and Assessment Project: Cape Cod Islands.* Massachusetts Department of Conservation and Recreation. Retrieved August 2020, from https://www.mass.gov/files/documents/2016/08/pd/vineyard-nantucket.pdf

Brayley, A. W. (1913). *History of the Granite Industry of New England.* Boston: E. L. Grimes Company. Retrieved August 2020, from https://play.google.com/books/reader?id=RasJAAAAIAAJ&hl=en&pg=GBS.PA94

Brennan, G. (2018, June 6). Norton Point latest area closed. *The Martha's Vineyard Times*. Retrieved from https://www.mvtimes.com/2018/06/06/norton-point-latest-area-closed/

Britannica, T. E. (2017, March 20). *Beaufort scale*. (Encyclopædia Britannica, inc.) Retrieved August 10, 2020, from Encyclopædia Britannica: https://www.britannica.com/science/Beaufort-scale

Brown, S. (2016, January 12). Two Days After Breach, Norton Point Beach Heals Again. *Vineyard Gazette*. Retrieved from https://vineyardgazette.com/news/2016/01/12/two-days-after-breach-norton-point-beach-heals-again

Buynevich, I. V., & Donnelly, J. P. (2006). Geological Signatures of Barrier Breaching and Overwash, Southern Massachusetts, USA. *Journal of Coastal Research*, 112-116. Retrieved from https://www.jstor.org/stable/25741544?casa_token=yWpzuViNJ9oAAAAA%3Ai5COubwpxv9n_NmAk-nrTpA4dqlDTjWuU0uC8GFBWvOMl43YdGIHiSw3Y8z0HX2QbmvLFZ1YdxOxN2Dk4zJDOzfv4PdvfVUkTV0kjbilGTNuY45iME31qA&seq=2#metadata_info_tab_contents

Campbell, T., Benedet, L., & Thomson, G. (2005, Spring). Design Considerations for Barrier Island Nourishments and Coastal Structures for Coastal Restoration in Louisiana. *Journal of Coastal Research*, 186-202. Retrieved from https://www.jstor.org/stable/pdf/25737057.pdf

Carruthers, E. A., Lane, D. P., Evans, R. L., Donnelly, J. P., & Ashton, A. D. (2013, September). Quantifying overwash flux in barrier systems: An example from Martha's Vineyard, Massachusetts, USA. *Marine Geology, 343*, 15-28. doi:10.1016/j.margeo.2013.05.013

CEDAS Details. (n.d.). Retrieved August 10, 2020, from Veritech Inc.: https://www.veritechinc.com/products/cedas/cedas-details

Church, J. A., & Clark, P. U. (2013). *Sea Level Change.* IPCC, Cambridge and New York. Retrieved from https://www.ipcc.ch/site/assets/uploads/2018/02/WG1AR5_Chapter13_FINAL.pdf

Dale, T. N. (1908). *The Chief Commerical Granites of Massachusetts, New Hampshire, and Rhode Island.* Washington: Government Printing Office. Retrieved from https://pubs.usgs.gov/bul/0354/report.pdf

Dale, T. N. (1923). *THE LIME BELT OF MASSACHUSETTS AND PARTS OF EASTERN NEW YORK.* Washington: USGS. Retrieved from https://pubs.usgs.gov/bul/0744/report.pdf

Davis, R. A., & Barnard, P. L. (2000, January 1). How anthropogenic factors in the back-barrier area influence tidal inlet stability: examples from the Gulf Coast of Florida, USA. *Geological Society Special Publications*, 293-303. doi:https://doi.org/10.1144/GSL.SP.2000.175.01.21

Dewhurst, T. (2013). Muskeget Channel tidal energy test facility. Retrieved from https://scholars.unh.edu/cgi/viewcontent.cgi?article=1794&context=thesis

Di Bona, S. (2013). *Modeling of Coastal Evolution: Long Term Simulation in the Vagueira Region (Portugal).* Retrieved from https://core.ac.uk/download/pdf/16697282.pdf

Dong, G. H., Zheng, Y. N., Li, Y. C., Teng, B., Guan, C. T., & Lin, D. F. (2008, June). Experiments on wave transmission coefficients of floating breakwaters. *Ocean Engineering*, 931-938. doi:10.1016/j.oceaneng.2008.01.010

Dunlop, T. (1999, July 30). Riches of Whaling Industry Came to Frigid End As Vineyard Captains Lost Ships Off Alaska. *Vineyard Gazette*. Retrieved from https://vineyardgazette.com/news/1999/07/30/riches-whaling-industry-came-frigid-end-vineyard-captains-lost-ships-alaska

Dunlop, T. (2011, May 1). An Eyewitness Account as the Beach Gives Way. *Martha's Vineyard Magazine*. Retrieved from https://mvmagazine.com/news/2011/05/01/eyewitness-account-beach-gives-way

Dunlop, T. (2011, May 1). Man's Efforts to Open – and Close – Norton Point. *Martha's Vineyard Magazine*. Retrieved from https://mvmagazine.com/news/2011/05/01/man%E2%80%99s-efforts-open-%E2%80%93-and-close-%E2%80%93-norton-point

Dunlop, T. (2011, May 1). Special Report: Norton Point Breach. *Martha's Vineyard Magazine*. Retrieved from https://mvmagazine.com/news/2011/05/01/special-report-norton-point-breach

Dunlop, T. (2011, May 1). The Norton of Norton Point. *Martha's Vineyard Magazine*. Retrieved from https://mvmagazine.com/news/2011/05/01/norton-norton-point

Dunlop, T. (2013, December 19). As Breach Retreats, Erosion Picks Up Speed. *Vineyard Gazette*. Retrieved from https://vineyardgazette.com/news/2013/12/19/breach-retreats-erosion-picks-speed

Dunlop, T. (2013, July 4). History and Science Tell of Cycles of Rapid Erosion at Wasque Point. *Vineyard Gazette*. Retrieved from https://vineyardgazette.com/news/2013/07/04/history-and-science-tell-cycles-rapid-erosion-wasque-point

Dunlop, T. (2014, February 21). *REVISED: A HISTORY OF THE OPENINGS (AND CLOSINGS).* Retrieved from Martha's Vineyard: A Meeting of Land And Sea: https://mvlandandsea.com/sites/default/files/Notes/7-NP-History_TomDunlop2014.pdf

Dunlop, T. (2015, October 18). Short-Lived Breach at Norton Point Closes. *Vineyard Gazette*. Retrieved from https://vineyardgazette.com/news/2015/10/18/short-lived-breach-norton-point-closes

Economic Profile of Martha's Vineyard. (n.d.). Retrieved August 11, 2020, from Martha's Vineyard Commission: https://www.mvcommission.org/economic-profile-marthas-vineyard

Eldrup, M., Lykke Andersen, T., & Burcharth, H. (2019). Stability of Rubble Mound Breakwaters—A Study of the Notional Permeability Factor, Based on Physical Model Tests. *Water*. doi:https://doi.org/10.3390/w11050934

Elvin, A. (2015, October 29). Breaches Carve a Path for Pond Management. *Vineyard Gazette*. Retrieved from https://vineyardgazette.com/news/2015/10/29/breaches-carve-path-pond-management

Elvin, A. (2015, April 23). Norton Point Breach Closing Benefits Birds, Shellfish. *Vineyard Gazette*. Retrieved from https://vineyardgazette.com/news/2015/04/23/norton-point-breach-closing-benefits-birds-shellfish

EXECUTIVE ORDER No. 181: Barrier Beaches (August 8, 1980). Retrieved from https://www.mass.gov/executive-orders/no-181-barrier-beaches

Federal Highway Administration. (2006). *ROCKERY DESIGN AND CONSTRUCTION GUIDELINES.* U.S. Department of Transportation. Retrieved from https://www.fhwa.dot.gov/clas/pdfs/RockeryDesignandConstructionGuidelines013007.pdf

Goff, J. A., Mayer, L. A., Traykovski, P., Buynevich, I., Wilkens, R., Raymond, R., . . . Jenkins, C. (2005, March). Detailed investigation of sorted bedforms, or "rippled scour depressions," within the Martha's Vineyard Coastal Observatory, Massachusetts. *Continental Shelf Research, 25*(4), 461-484. doi:10.1016/j.csr.2004.09.019

Google Earth. (2005-2015). Norton Point Beach in Edgartown, MA. Retrieved April 3, 2000

Google Earth. (2018-2020). Eastern United States, Massachusetts, Edgartown, and Southeastern Edgartown. Retrieved August 10, 2020

Gravens, M. B., Kraus, N. C., & Hanson, H. (1991). *GENESIS: GENERALIZED MODEL FOR SIMULATING SHORELINE CHANGE, REPORT 2, WORKBOOK AND SYSTEM USER'S MANUAL.* Army Corps of Engineers. Retrieved from https://apps.dtic.mil/dtic/tr/fulltext/u2/a241748.pdf

Guler, H., Ergin, A., & Ozyurt Tarakcioglu, G. (2014, January). A COMPARATIVE STUDY ON THE STABILITY FORMULAS OF RUBBLE MOUND BREAKWATERS. *Coastal Engineering Proceedings*. doi:10.9753/icce.v34.structures.27

Hanson, H., & Kraus, N. (2004, Winter). Advancements in One-Line Modeling of T-Head Groins: (Genesis-T). *Journal of Coastal Research*, 315-323. Retrieved from https://www.jstor.org/stable/25736262

Harrison, M. (2010, June 1). Drive Along the Beach Road. *Our State*. Retrieved from https://www.ourstate.com/nc-highway-12/

Hedges, T. S. (n.d.). *Wave Breaking and Reflection*. Retrieved from ENSEEIHT: http://hmf.enseeiht.fr/travaux/CD0102/travaux/optsee/bei/2/g2s/Wave_Breaking_and_Reflection.pdf

Hurricane Bob Roared, and Martha's Vineyard Shook. (2016, August 18). *Vineyard Gazette*. doi:https://vineyardgazette.com/news/2016/08/18/hurricane-bob-roared-and-marthas-vineyard-shook

Inlets. (n.d.). Retrieved from Intro to Coasts: http://w3.salemstate.edu/~lhanson/gls210/GLS210_coasts/inlets.htm

Katama Bay Oysters. (n.d.). Retrieved from J.P.'s Shellfish: https://www.jpshellfish.com/oysters/katama-bay-oysters/

Kraus, N. C., Larson, M., & Wise, R. A. (n.d.). *Depth of Closure in Beach-fill Design.* U.S. Army Engineer Waterways Experiment Station. Retrieved from https://apps.dtic.mil/dtic/tr/fulltext/u2/a578584.pdf

Landsat Images on Glovies. (2018). Retrieved from USGS: https://glovis.usgs.gov/app?fullscreen

Landsat Images on GloVis. (1991). Retrieved from USGS: https://glovis.usgs.gov/app?fullscreen=0

Landsat Images on Glovis. (2018). Retrieved from USGS: https://glovis.usgs.gov/app?fullscreen

Lee, W.-D., Jeong, Y.-M., & Hur, D.-S. (2019, December). Wave Control by Tide-Adapting Submerged Breakwater. *Journal of Ocean Engineering and Technology, 33*(6). doi:10.26748/KSOE.2019.081

Lovewell, M. A. (2005, February 24). Edgartown Officials Stand Firm on Katama Bay Anchorage Ban. *Vineyard Gazette*. Retrieved from https://vineyardgazette.com/news/2005/02/25/edgartown-officials-stand-firm-katama-bay-anchorage-ban

Mangor, K., Drønen, N. K., Kristensen, S. E., & Kaergaard, K. H. (2017). *Shoreline Management Guidelines.* DHI. Retrieved from https://www.dhigroup.com/upload/campaigns/ShorelineManagementGuidelines_Feb2017.pdf

Massachusetts Shoreline Change Browser. (n.d.). (Massachusetts Office of Coastal Zone Management) Retrieved July 2020, from Mass.gov: http://maps.massgis.state.ma.us/map_ol/czm_shorelines.php

McCartney, B. L. (1985). Floating Breakwater Design. *Journal of Waterway, Port, Coastal, and Ocean Engineering, 111*(2). doi:10.1061/(ASCE)0733-950X(1985)111:2(304)

Moon Phases Calendar. (n.d.). Retrieved from The University of Arizona Lunar and Planetary Laboratory: https://catalina.lpl.arizona.edu/moon/phases/calendar?month=4&year=2007

New York State Department of Environmental Conservation. (n.d.). *Protection against Wavebased Erosion.* Retrieved from https://www.dec.ny.gov/docs/water_pdf/waverosionrevetment.pdf

NIWA. (2004). *Wave Energy Coastal Waves Primer.* Wellington, New Zealand: National Institute of Water & Atmospheric Research Ltd. Retrieved from http://docs.niwa.co.nz/library/public/waveprimer.pdf

NOAA. (2007). *Heavy Rains & Significant Snows: April 15-16,2007*. Retrieved from ERH: NOAA: http://www.erh.noaa.gov/er/aly/Past/2007/Apr_15-16_2007/Apr_15-16_2007.htm [https://web.archive.org/web/20150924002103/http://www.erh.noaa.gov/er/aly/Past/2007/Apr_15-16_2007/Apr_15-16_2007.htm]

NOAA. (2019). *Sea Level Rise Viewer*. Retrieved from Office of Coastal Management: https://coast.noaa.gov/digitalcoast/tools/slr.html

NOAA. (2020). *Relative Sea Level Trend: 8449130 Nantucket Island, Massachusetts*. Retrieved from Tides and Currents: https://tidesandcurrents.noaa.gov/sltrends/sltrends_station.shtml?id=8449130

PIANC. (2003). *MarCom WG 40: State-of-the-Art of Designing and Constructing Berm Breakwaters.* PIANC. Retrieved from https://www.kennisbank-waterbouw.nl/breakwaters/reference/BRKref184.pdf

Previsic, M. (2016). *System Level Design, Performance, Cost, and Economic Assessment – Massachusetts Muskeget Channel Tidal In-Stream Power Plant.* EPRI. Retrieved from http://www.re-vision.net/documents/System%20Level%20Design,%20Performance,%20Cost%20and%20Economic%20Assessment%20-%20Massachusetts%20Muskeget%20Channel%20Tidal%20In-Stream%20Power%

Seabrook, S. R., & Hall, K. R. (1998). *Wave Transmission at Submerged Rubblemound Breakwaters.* 26th International Conference on Coastal Engineering. doi:https://doi.org/10.1061/9780784404119.150

Sigurdarson, S., Smarason, O., Viggosson, G., & Bjørdal, S. (2006). WAVE HEIGHT LIMITS FOR THE STATICALLY STABLE ICELANDIC-TYPE BERM BREAKWATER ICELANDIC-TYPE BERM BREAKWATER. doi:10.13140/2.1.3509.1207

Takahashi, S. (2002). *Design of Vertical Breakwaters.* PORT AND AIRPORT RESEARCH INSTITUTE. Retrieved from https://pdfs.semanticscholar.org/bab3/715070c06a6daf4f93b7101c755d92d05cd3.pdf

The M.W. Kellogg Company. (1972). *Availability of Limestones and Dolomites: Task #1 Final Report.* Retrieved from https://nepis.epa.gov/Exe/ZyPURL.cgi?Dockey =9100246I.TXT

Tidal Currents through Vineyard and Nantucket Sounds. (2003). (B. R. Hall, Compiler) Retrieved from https://www.digitalcommonwealth.org/search/commonwealth: vh53xt772

Uda, T., Serizawa, M., & Miyahara, S. (2018). Formation of Sand Spit and Bay Barrier. In *Morphodynamic Model for Predicting Beach Changes Based on Bagnold's Concept and Its Applications* (p. 1). Tokyo: IntechOpen. doi:10.5772/ intechopen.81415

US Army Corps of Engineers. (2003). Surf Zones Hydrodynamics. In *Coastal Engineering Manual, Part II, Chapter II-4.* Washington D.C.

USGS, NOAA. (n.d.). Map of Edgartown, MA Tidal Gauge Location. Retrieved August 11, 2020, from https://tidesandcurrents.noaa.gov/stationhome.html?id=8448558

USGS, NOAA. (n.d.). Map of Nantucket Island, MA Tidal Gauge Location. Retrieved August 10, 2020, from https://tidesandcurrents.noaa.gov/stationhome.html ?id=8449130

Van der Meer, J. W. (1988) "Rock Slopes and Gravel Beaches under Wave Attack", Ph.D. Thesis, Delft University, the Netherlands. Retrieved from https://pdfs. semanticscholar.org/039c/82065e4e5afe2705b97ae3d25cdc0efd3dd9.pdf

Velasquez Montoya, L., Sciaudone, E. J., Mitasova, H., & Overton, M. F. (2018, March 15). Observation and modeling of the evolution of an ephemeral storm-induced inlet: Pea Island Breach, North Carolina, USA. *Continental Shelf Research, 156*, 55-69. doi:10.1016/j.csr.2018.02.002

Waterways Experiment Station. (1953). *Stability of Rubble-Mound Breakwaters.* Army Corps of Engineers. Retrieved from https://usace.contentdm.oclc.org/digital/api/ collection/p266001coll1/id/1703/download

Weight Per Cubic Foot And Specific Gravity (Typical). (2020). Retrieved from Reade: https://www.reade.com/reade-resources/reference-educational/reade-reference-chart-particle-property-briefings/26-weight-per-cubic-foot-and-specific-gravity-metals-minerals-organics-inorganics-ceraqmics

Wells, J. (2016, January 10). Norton Point Breaks Open Again on Stormy, Windswept Day. *Vineyard Gazette*. Retrieved from https://vineyardgazette.com/news/2016/01/ 10/norton-point-breaks-open-again-stormy-windswept-day?k=vg54a3f87b53c75

Wells, J. (2018, March 3). Northeaster Leaves Island in Cleanup Mode. *Vineyard Gazette*. Retrieved from https://vineyardgazette.com/news/2018/03/03/severe-northeaster-leaves-island-cleanup-mode

WHOI. (2020). *Infrastructure*. Retrieved from Martha's Vineyard Coastal Observatory: https://mvco.whoi.edu/infrastructure/

World of Page: Coastline Change. (n.d.). Retrieved from NASA Earth Observatory: https://earthobservatory.nasa.gov/world-of-change/CapeCod